PL-embedding the dual of two Jordan curves into $\mathbb{S}^3$ by an $O(n^2)$-algorithm *

Sóstenes Lins and Ricardo Machado

July 8, 2013

Abstract

Let be given a *colored 3-pseudo-triangulation* $\mathcal{H}^\star$ with n tetrahedra. Colored means that each tetrahedron have vertices distinctively colored 0,1,2,3. In a *pseudo* 3-triangulation the intersection of simplices might be subsets of simplices of smaller dimensions (faces), instead of a single maximal face, as for true triangulations. If $\mathcal{H}^\star$ is the dual of a cell 3-complex induced (in an specific way to be made clear) by a pair of Jordan curves with $2n$ transversal crossings, then we show that the induced 3-manifold $|\mathcal{H}^\star|$ is $\mathbb{S}^3$ and we make available an $O(n^2)$-algorithm to produce a PL-embedding ([12]) of $\mathcal{H}^\star$ into $\mathbb{S}^3$. This bound is rather surprising because such PL-embeddings are often of exponential size. This work is the first step towards obtaining, via an $O(n^2)$-algorithm, a framed link presentation inducing the same closed orientable 3-manifold as the one given by a colored pseudo-triangulation. Previous work on this topic appear in [9], [10] and [11]. However, the exposition and the new proofs of this paper are meant to be entirely self-contained.

1 Introduction

1.1 J^2-gems

A J^2*-gem* is a 4-regular, 4-edge-colored planar graph $\mathcal{H}$ obtained from the intersection pattern of two Jordan curves X and Y with $2n$ transversal crossings. These crossings define consecutive segments of X alternatively inside Y and outside Y. Color the first type 2 and the second type 3. The crossings also define consecutive segments of Y alternatively inside X and outside X. Color the first type 0 and the second type 1. This defines a 4-regular 4-edge-colored graph $\mathcal{H}$ where the vertices are the crossings and the edges are the colored colored segments. Let $\mathcal{H}^\star$ be the 3-dimensional abstract 3-complex formed by taking a set of vertex colored tetrahedra in 1–1 correspondence with the set of vertices of $\mathcal{H}$, $V(\mathcal{H})$, so that each tetrahedra has vertices of colors 0,1,2,3. This vertex coloring induces a face coloring of the triangular faces of the tetrahedron: color i the face opposite to the vertex colored i. For each i-colored edge of $\mathcal{H}$ with ends u and v paste the corresponding tetrahedra ∇_u and ∇_v so as to paste the two triangular faces that do not contain a vertex of color i in such a way as to to match vertices of the other three colors. We show that the topological space $|K|$ induced by $\mathcal{H}^\star$ is $\mathbb{S}^3$. Moreover we describe an $O(n^2)$-algorithm to

*2010 Mathematics Subject Classification: 57M25 and 57Q15 (primary), 57M27 and 57M15 (secondary) make available a PL-embedding ([12]) of $\mathcal{H}^\star$ into $\mathbb{S}^3$. We get explicit coordinates in $\mathbb{S}^3$ for the 0-simplices and the p-simplices ($p \in \{1, 2, 3\}$) become linear simplices in the spherical geometry. For basic topological definitions we refer to the lucid book by Stillwell [13].

1.2 Gems and their duals

A *(3+1)-graph* $\mathcal{H}$ is a connected regular graph of degree 4 where to each vertex there are four incident differently colored edges in the color set $\{0, 1, 2, 3\}$. For $I \subseteq \{0, 1, 2, 3\}$, an *I-residue* is a component of the subgraph induced by the I-colored edges. Denote by $v(\mathcal{H})$ the number of 0-residues (vertices) of $\mathcal{H}$. For $0 \le i < j \le 3$, an $\{i, j\}$-residue is also called an *ij-gon* or an i- and j-colored *bigon* (it is an even polygon, where the edges are alternatively colored i and j). Denote by $b(\mathcal{H})$ the total number of ij-gons for $0 \le i < j \le 3$. Denote by $t(\mathcal{H})$ the total number of $\bar{i}$-residues for $0 \le i \le 3$, where $\bar{i}$ means complement of $\{i\}$ in $\{0, 1, 2, 3\}$.

We briefly recall the definition of gems taken from [8]. A 3-*gem* is a $(3 + 1)$-graph $\mathcal{H}$ satisfying $v(\mathcal{H}) + t(\mathcal{H}) = b(\mathcal{H})$. This relation is equivalent to having the vertices, edges and bigons restricted to any $\{i, j, k\}$-residue inducing a plane graph where the faces are bounded by the bigons. Therefore we can embed each such $\{i, j, k\}$-residue into a sphere $\mathbb{S}^2$. We consider the ball bounded this $\mathbb{S}^2$ as induced by the $\{i, j, k\}$-residue. For this reason an $\{i, j, k\}$-residue in a 3-gem, $i < j < k$, is also called a *triball.* An ij-gon appears once in the boundary of triball $\{i, j, k\}$ and once in the boundary of triball $\{i, j, h\}$. By pasting the triballs along disks bounded by all the pairs of ij-gons, $\{i, j\} \subset \{0, 1, 2, 3\}$ of a gem $\mathcal{H}$, we obtain a closed 3-manifold denoted by $|\mathcal{H}|$. This general construction is dual to the one exemplified in the abstract and produces any closed 3-manifold. The manifold is orientable if and only if $\mathcal{H}$ is bipartite, [6]. A *crystallization* is a gem which remains connected after deleting all the edges of any given color, that is, it has one $\{i, j, k\}$-residue for each trio of colors $\{i, j, k\} \subset \{0, 1, 2, 3\}$.

Let $\mathcal{H}^\star$ be the dual of a gem $\mathcal{H}$. An $\bar{i}$-residue of $\mathcal{H}$ corresponds in $\mathcal{H}^\star$ to a 0-simplex of $\mathcal{H}^\star$. Most 0-simplices of $\mathcal{H}^\star$ do not correspond to $\bar{i}$-residues of $\mathcal{H}$. An ij-gon of a gem $\mathcal{H}$ corresponds in $\mathcal{H}^\star$ to a *PL1-face* formed by a sequence of 1-simplices of $\mathcal{H}^\star$; this PL1-face is the intersection of two PL2-faces of colors i and j; their two bounding 0-simplices correspond to an $\bar{h}$- and to a $\bar{k}$-residue, where $\{h, i, j, k\} = \{0, 1, 2, 3\}$. An i-colored edge of $\mathcal{H}$ corresponds to a *PL2-face* which is a 2-disk triangulated by a subset of i-colored 2-simplices of $\mathcal{H}^\star$. Finally to a vertex of $\mathcal{H}$, it corresponds a *PL3-face* of $\mathcal{H}^\star$ which is a 3-ball formed by a subset of 3-simplices of $\mathcal{H}^\star$.

(1.1) Proposition. *The* 3*-manifold induced by a* J^2*-gem* $\mathcal{H}$ *is* $\mathbb{S}^3$*.*

Proof. Removing from $\mathcal{H}$ all the edges of a given color still yields a connected graph which a plane graph and they come embedded so that the faces are the 2-residues. So $\mathcal{H}$ has four 3-residues, one of each type. Denote by b_{ij} the number of ij-gons of $\mathcal{H}$. Each one of these residues are planar graphs having $v = 2n$ vertices, $3v/2$ edges and $b_{12} + b_{13} + b_{23}$, $b_{02} + b_{03} + b_{23}$, $b_{01} + b_{13} + b_{03}$ and $b_{12} + b_{01} + b_{02}$ faces for, respectively, the $\bar{0}$-, $\bar{1}$-, $\bar{2}$-, $\bar{3}$-residue. Adding the four formulas for the Euler characteristic of the sphere imply that $v(\mathcal{H}) + 4 = b(\mathcal{H})$. Therefore, $\mathcal{H}$ is a crystallization having one $0i$-gon and one jk-gon. This implies that the fundamental group of the induced manifold is trivial: as proved in [5], the fundamental group of the space induced by a crystallization is generated by $b_{0i} - 1$ generators, and in our case this number is 0. Since Poincaré Conjecture is now proved, we are done. However, we can avoid using this fact and, as a bonus, obtaining the validity of the next corollary, which is used in the sequel.

Assume that $\mathcal{H}$ is a J^2-gem which does not induce $\mathbb{S}^3$ and has the smallest possible number of vertices satisfying these assumptions. By planarity we must have a pair of edges of $\mathcal{H}$ having the same ends $\{p, q\}$. Consider the graph $\mathcal{H}fus\{p, q\}$ obtained from $\mathcal{H}$ by removing the vertices p, q and the 2 edges linking them as well as welding the 2 pairs of pendant edges along edges of the same color. In [4] S. Lins proves that if $\mathcal{H}$ is a gem, $\mathcal{H}' = \mathcal{H}fus\{p, q\}$ is also a gem and that two exclusive relations hold regarding $|\mathcal{H}|$ and $|\mathcal{H}'|$, their induced 3-manifolds: either $|\mathcal{H}| = |\mathcal{H}'|$ in the case that $\{p, q\}$ induces a 2-dipole or else $|\mathcal{H}| = |\mathcal{H}'|\#(\mathbb{S}^2 \times \mathbb{S}^1)$. Since $\mathcal{H}'$ is a J^2-gem, by our minimality hypothesis on $\mathcal{H}$ the valid alternative is the second. But this is a contradiction: the fundamental group of $|\mathcal{H}|$ would not be trivial, because of the summand $\mathbb{S}^2 \times \mathbb{S}^1$. □

1.3 Dipoles, pillows and balloons

Suppose there are m edges linking vertices x and y of a gem, $m \in \{1, 2, 3\}$. We say that $\{u, v\}$ is an *m-dipole* if removing all edges in the colors of the ones linking x to y, these vertices are in distinct components of the graph induced by the edges in the complementary set of colors. To *cancel the dipole* means deleting the subgraph induced by $\{u, v\}$ and identify pairs of the hanging edges along the same remaining color. To *create the dipole* is the inverse operation. It is simple to prove that the manifold of a gem is invariant under dipole cancellation or creation. Even though is not relevant for the present work state the foundational result on gems: two 3-manifolds are homeomorphic if and only if any two gems inducing it are linked by a finite number of cancellations and creations of dipoles, [3, 7].

The dual of a 2-dipole $\{u, v\}$, with internal colors i, j is named a *pillow*. It consistes of two PL3-faces ∇_u and ∇_v sharing two PL2-faces colored i and j. The *thickening of a 2-dipole into a 3-dipole* is defined as follows. Let i, j be the two colors internal to 2-dipole $\{u, v\}$ and k a third color. Let a be the k-neighboor of x and b be the k-neighboor of y. Remove edges $[a, x]$ and $[b, y]$ and put back k-edges $[u, v]$ and $[r, s]$. This completes the thickening. It is simple to prove that the thickening in a gem produces a gem. We must be carefull because the inverse blind inverse operation *thinning a 3-dipole* not always produces a gem. The catch is that the result of the thinning perhaps is not a 2-dipole. In this sense the thinning move is not local: we must make sure that the result is a 2-dipole. To the data needed in thinning a 3-dipole $\{u, v\}$ with internal colors $\{i, j, k\}$ we must add the k-edge $[r, s]$. Note that the k-edges $[u, v]$ and $[r, s]$ are in the same hk-gon, where h is the fourth color. Denote by Δ_{rs} the dual of $[r, s]$. Let $\nabla_u \cup \nabla v \cup \Delta_{rs}$ be called a *balloon*. Note that it consists of 2 PL3-faces ∇_u and ∇_v sharing three PL2-faces in colors $\{i, j, k\}$ together with a k-colored PL2-face whose intersection with $\nabla_u \cup \nabla_v$ is a PL1-face corresponding to the dual of the hk-gon, where h is the fourth color. Let $\nabla_u \cup \nabla_v$ be the *balloon's head* and let Δ_{rs} be the *balloon's tail*.

1.4 The Strategy for finding the $O(n^2)$-algorithm

We want to find a PL-embedding for the dual $\mathcal{H}^\star$ of a J^2-gem $\mathcal{H}$ into $\mathbb{S}^3$. To this end we remove one PL3-face of $\mathcal{H}^\star$ (one vertex of $\mathcal{H}$) and find a PL-embedding in $\mathbb{R}^3$ forming a a PL-triangulated tetrahedron. After we use the inverse of a stereographic projection with center in the exterior of the triangulated tetrahedron. In this way we recover in $\mathbb{S}^3$ the missing PL3-face.

In this work we describe the PL-embedded PL3-faces of $\mathcal{H}^\star$ into $\mathbb{R}^3$ by making it geometrically clear that its boundary is a set of 4 PL2-faces, one of each color, forming an embedded $\mathbb{S}^2$ whose interior is disjoint from the interior of $\mathbb{S}^2$'s corresponding to others PL3-faces. Thus, for our purposes it will be only necessary to embed the 2-skeleton of $\mathcal{H}^\star$.

A direct approach to find the PL-embedding of the dual of a general J^2-gem with $2n$ vertices, seems very hard. Therefore, we split the algorithm into 4 phases.

In the first phase we find a sequence of $n-1$ 2-dipole thickenings into 3-dipoles not using color 3, where the new involved edge is either 0 or 1 so that the final gem is simply a circular arrangement of n 3-dipoles with internal colors $0, 1, 2$. Such a canonical n-gem is named a *bloboid* and is denoted $\mathcal{B}_n$. Such 3-dipoles are also named a *blob over a 3-colored edge.* A J^2B-gem is a gem that, after cancelling blobs over 3-colored edge becomes a J^2-gem. This indexing decreasing sequence is easily obtainable from the primal objects, in the case, simplifying J^2B-gems until the bloboid is obtained:

$$\mathcal{H} = \mathcal{H}_n \xrightarrow[thick_1]{2dip} \mathcal{H}_{n-1} \xrightarrow[thick_2]{2dip} \dots \xrightarrow[thick_{n-1}]{2dip} \mathcal{H}_1 = \mathcal{B}_n = \mathcal{B}.$$

In the second phase we first find (phase 2A) specific abstract PL-triangulations, for the PL2-faces for the index increasing sequence of abstract colored 2-dimensional PL-complexes. Each of these complexes, latter, are going to be PL-embedded into $\mathbb{R}^3$ so that the PL2-faces are topologically 2-spheres with disjoint interior. Attaching 3-balls bounded by these spheres we get the dual of the J^2-gem $\mathcal{H}$ (with a vertex removed).

$$\mathcal{B}^\star = \mathcal{H}_1^\star \xrightarrow[move_1]{bp} \mathcal{H}_2^\star \xrightarrow[move_2]{bp} \dots \xrightarrow[move_{n-1}]{bp} \mathcal{H}_n^\star = \mathcal{H}^\star.$$

In parallel to the construction of the sequence $\mathcal{H}_m^\star$'s we also construct (phase 2B) a sequence of *wings* $\mathcal{W}_m$'s and their *nervures* $\mathcal{N}_m$'s so that $\mathcal{S}_m = \mathcal{W}_m \cup \mathcal{N}_m$, called *a strut*, is an adequate planar graph, defined recursively. Moreover, wings and nervures are partitioned into their *left* and *right* parts: $\mathcal{W}_m = \mathcal{W}'_m \cup \mathcal{W}''_m$ and $\mathcal{N}_m = \mathcal{N}'_m \cup \mathcal{N}''_m$. The sequence of struts is

$$\mathcal{S}_1^\star = \mathcal{W}_1 \cup \mathcal{N}_1 \xrightarrow[move_1]{wbp} \mathcal{S}_2^\star = \mathcal{W}_2 \cup \mathcal{N}_2 \xrightarrow[move_2]{wbp} \dots \xrightarrow[move_{n-1}]{wbp} \mathcal{S}_n^\star = \mathcal{W}_n \cup \mathcal{N}_n = \mathcal{W} \cup \mathcal{N} = \mathcal{S}^\star.$$

Each wing $\mathcal{W}_m$'s corresponds to a section of the previous sequence $\mathcal{H}_m^\star$'s by two adequated fixed semi-planes Π' and Π''. The construction of the struts (which are planar graphs) is recursive. Initially $\mathcal{W}_1^\star$ is a pincel of lines and $\mathcal{N}_1^\star$ is $\varnothing$. Going from $\mathcal{S}_m^\star$ to $\mathcal{S}_{m+1}^\star$ is very simple: two new vertices and four new edges appear, so as to maintain planarity.

In the third phase we make the abstract final element $\mathcal{W}^\star \cup \mathcal{N}^\star$ of the second phase *rectilinearly* (that is each edge is a straihgt line segment) PL-embedded. By a cone construction we obtain from the rectilinearly PL-embedded strut $\mathcal{S}^\star$ a special PL-complex, named $\mathcal{H}_1^\diamond$. This complex does not correpond to a gem dual and it can be loosely explained as $\mathcal{H}_1^\star$ with all balloon's heads "opened".

The fourth phase, the *pillow filling phase* starts with $\mathcal{H}_1^\diamond$ and the uses the abstract sequence $\mathcal{H}_m^\star$'s to produce a pillow filling sequence

$$\mathcal{H}_1^\diamond \xrightarrow[filling_1]{pillow} \mathcal{H}_2^\diamond \xrightarrow[filling_2]{pillow} \dots \xrightarrow[filling_{n-1}]{pillow} \mathcal{H}_n^\diamond = \mathcal{H}^\star.$$

In this phase everything is embedded into $\mathbb{R}^3$ and the last element, $\mathcal{H}^\star$, is the PL-embedding that we seek: the PL-embedding of the dual of the original J^2-gem $\mathcal{H}$ minus a vertex into $\mathbb{R}^3$.

The whole procedure can be implemented as a formal algorithm that takes $O(n^2)$-space and $O(n^2)$-time complexity, where $2n$ is the number of vertices of the original J^2-gem.

1.5 A complete example

In the example coming from r_5^{24} (Figs. 1 to 6) we gather and display the data structure we need for the $O(n^2)$-algorithm to PL-embed the dual of a J^2-gem. The wings, nervures and their union the struts are partitioned into left and right parts:

$$\mathcal{W}_m = \mathcal{W}'_m \cup \mathcal{W}''_m, \quad \mathcal{N}_m = \mathcal{N}'_m \cup \mathcal{N}''_m, \quad \mathcal{S}^\star_m = \mathcal{S}^{\star'}_m \cup \mathcal{N}''_m,$$

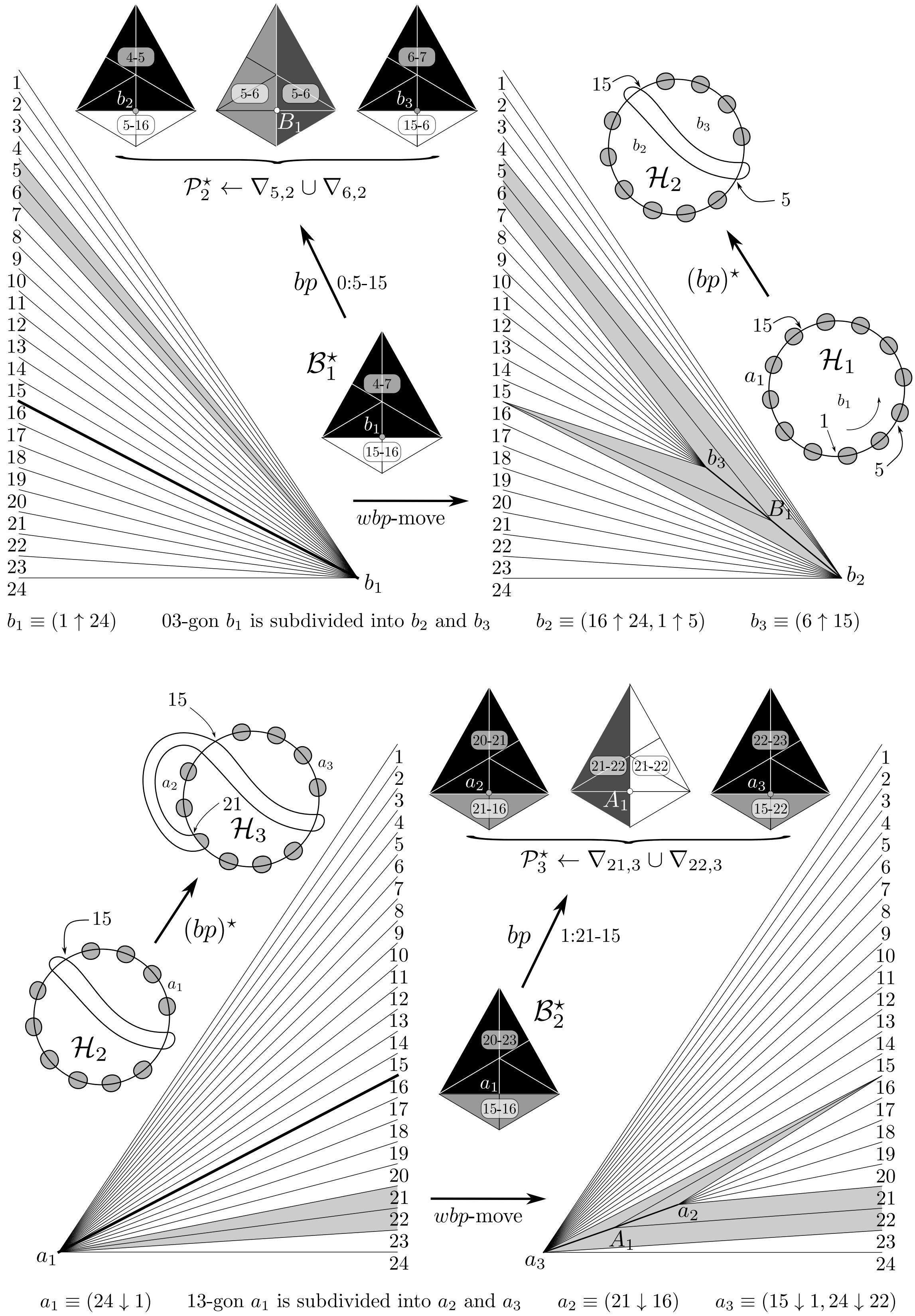

Figure 1: The initial right wing $\mathcal{W}_1''$ is a pincel of lines emanating from b_1. The initial right nervure $\mathcal{N}_1''$ is empty. The initial left wing $\mathcal{W}_1'$ is a pincel of lines emanating from a_1. The initial left nervure $\mathcal{N}_1'$ is empty. At the end of each wpb-move a pair of edges is added to the nervure. Lower case symbols a_j, b_k refer to 13-gons and 03-gons. Upper case symbols A_j, B_k are auxiliary 0-simplexes.

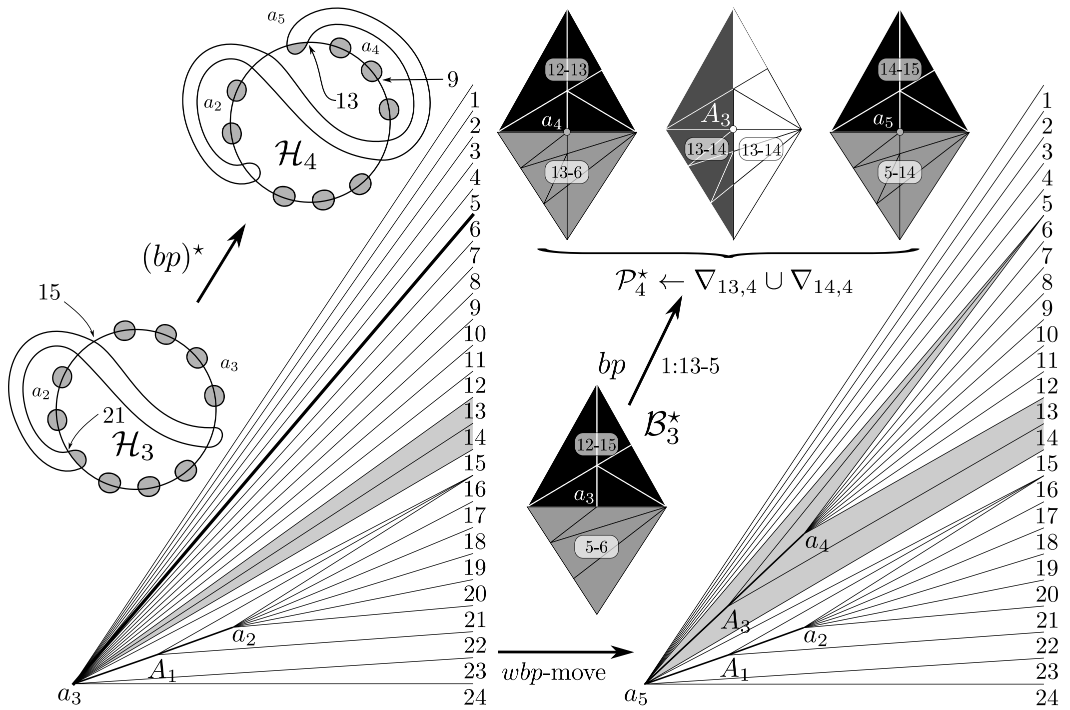

13-gon a_3 is subdivided into a_4 and a_5 $a_2 \equiv (21 \downarrow 16)$ $a_4 \equiv (13 \downarrow 6)$ $a_5 \equiv (15, 14, 5 \downarrow 1, 24 \downarrow 22)$

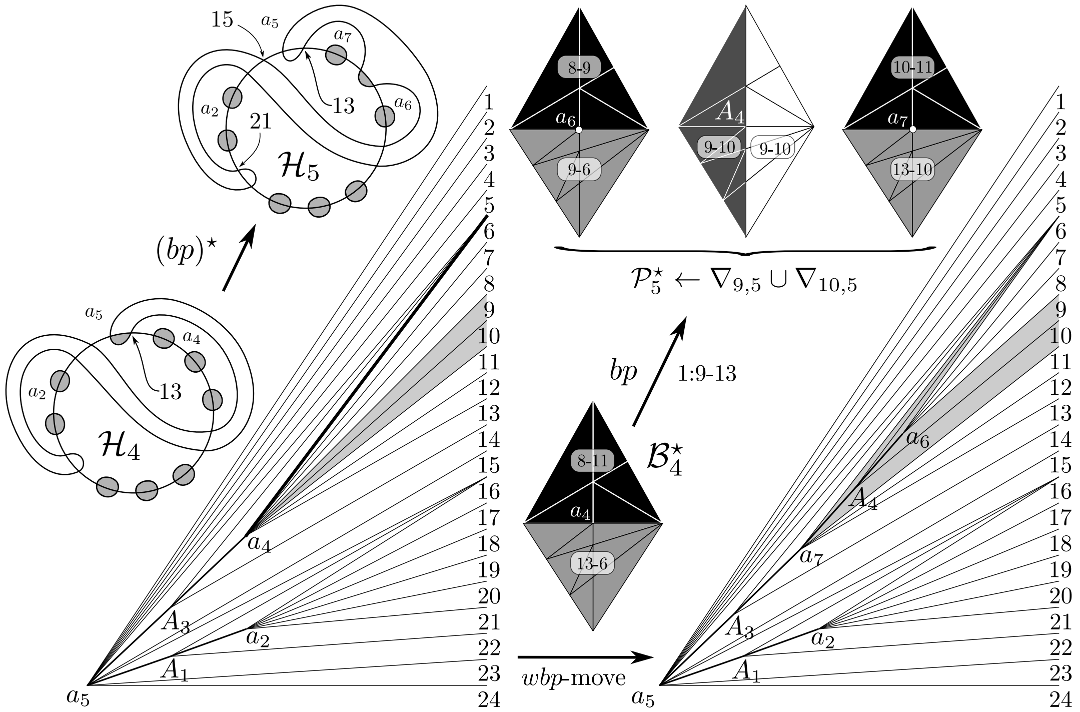

13-gon a_4 is subdivided into a_6 and a_7 $a_2 \equiv (21 \downarrow 16)$ $a_5 \equiv (15, 14, 5 \downarrow 1, 24 \downarrow 22)$ $a_6 \equiv (9 \downarrow 6)$ $a_7 \equiv (13 \downarrow 10)$

Figure 2: A left strut is modified by a wbp-move. What is needed as input is a pair of adjacent shaded triangles and a thick edge. In the lower the left strut is further modified by another wbp-move. The modification of balloons into pillows define the new colored abstract combinatorial complexes. The nervures $\mathcal{N}_m$ are auxiliar devices that will be disposed after we find the rectilinear embedded $\mathcal{W}$ by a deterministic linear algorithm, See Fig. 6.

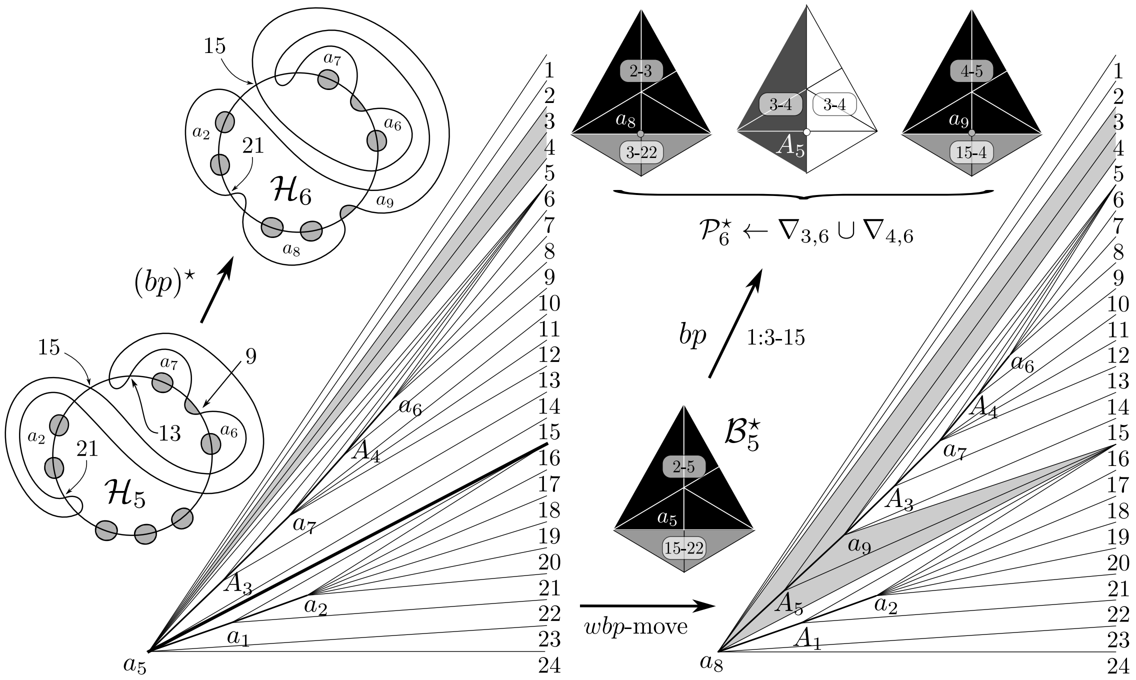

13-gon a_5 is subdivided into a_8 and a_9 $\quad a_2 \equiv (21 \downarrow 16) \quad a_6 \equiv (9 \downarrow 6) \quad a_7 \equiv (13 \downarrow 10) \quad a_8 \equiv (3 \downarrow 1, 24 \downarrow 22)$
$a_9 \equiv (15, 14, 5, 4)$

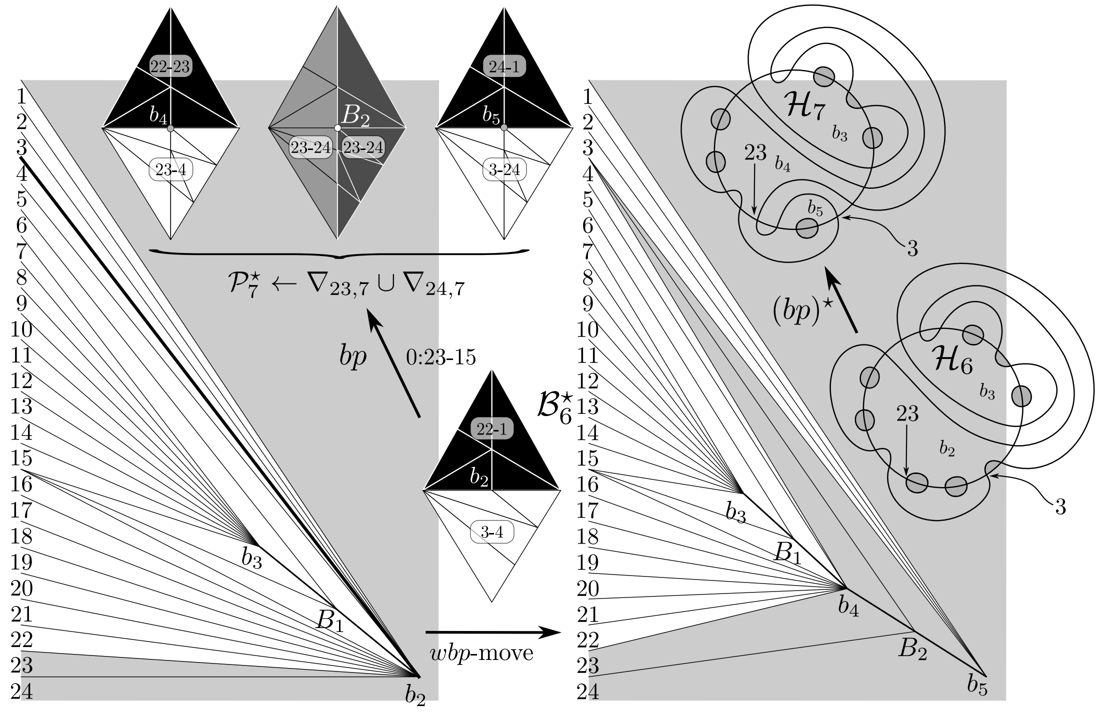

03-gon b_2 is subdivided into b_4 and b_5 $\quad b_3 \equiv (6 \uparrow 15) \quad b_4 \equiv (16 \uparrow 23, 4, 5) \quad b_5 \equiv (24, 1 \uparrow 3)$

Figure 3: In the first wbp-move a left strut is *extended based on* a_5. In all the figures of this r_5^{24}-example (except for the $\mathcal{W}$ at the last one) we have used Tutte's barycentric method [14, 1] to obtain the embedded final struts. However, except for $\mathcal{W}$, only the combinatorics of the embeddings (the rotations) are needed to encode the struts in an implementation of the algorithm. In the second wbp-move one of the two shaded triangles is in the outside. Depite this special case, the rotation manifestation of the move behaves as usual.

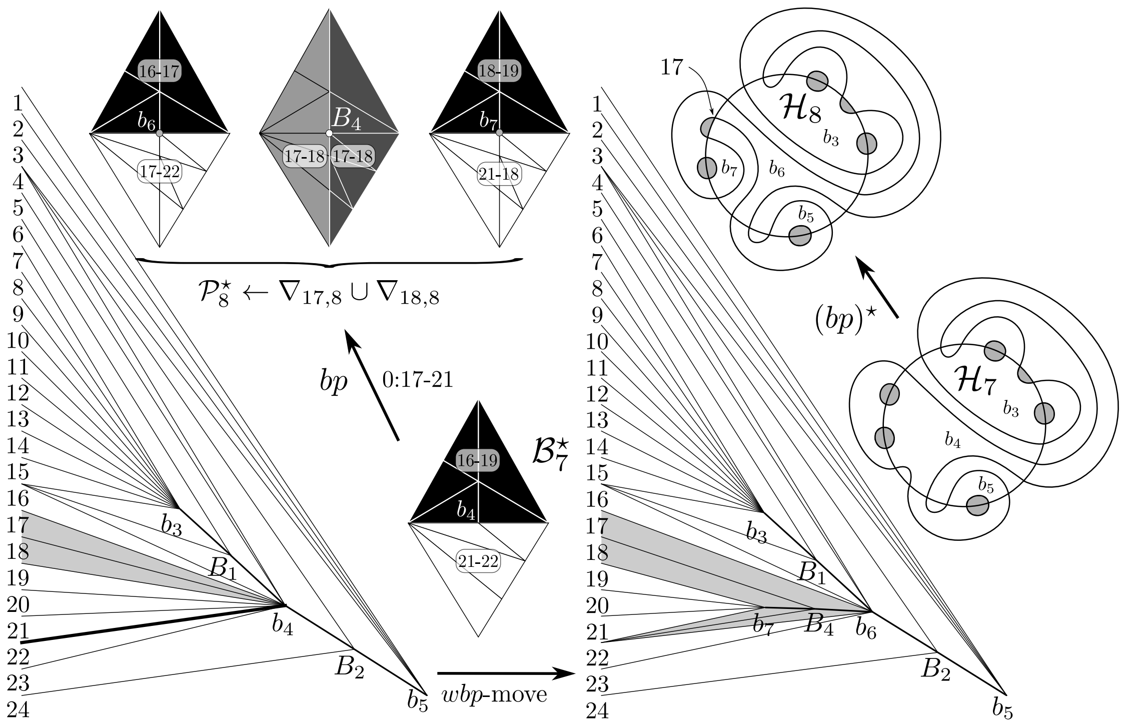

03-gon b_4 is subdivided into b_6 and b_7 $b_3 \equiv (6 \uparrow 15)$ $b_5 \equiv (24, 1 \uparrow 3)$ $b_6 \equiv (16, 17, 22, 23, 4, 5)$
$b_7 \equiv (18 \uparrow 21)$

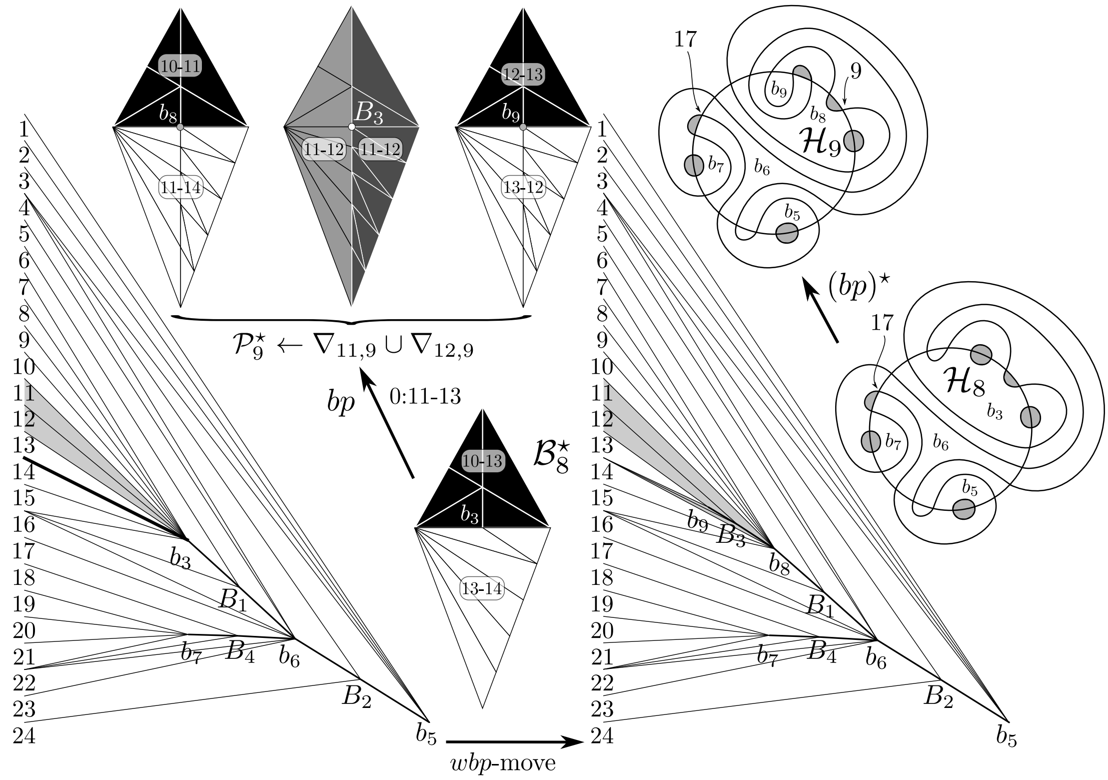

03-gon b_3 is subdivided into b_8 and b_9 $b_5 \equiv (24, 1 \uparrow 3)$ $b_6 \equiv (16, 17, 22, 23, 4, 5)$ $b_7 \equiv (18 \uparrow 21)$
$b_9 \equiv (12, 13)$ $b_8 \equiv (6 \uparrow 10, 11, 14, 15)$

Figure 4: The first wbp-move induces a bifurcation on the nervure of a right wing based on b_4. The second wbp-move produces an extension based on b_3 of the nervure of the final right wing of the first wbp-move.

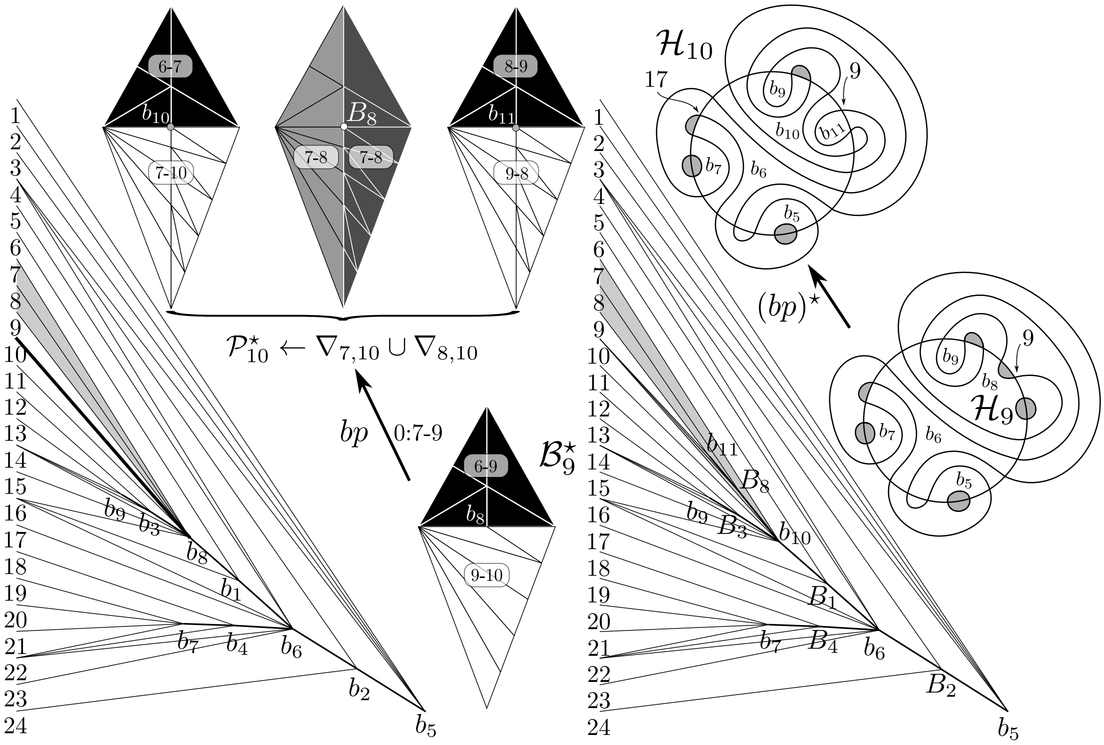

03-gon b_8 is subdivided into b_{10} and b_{11} $b_5 \equiv (24, 1 \uparrow 3)$ $b_6 \equiv (16, 17, 22, 23, 4, 5)$ $b_7 \equiv (18 \uparrow 21)$
$b_{10} \equiv (15, 6, 7, 10, 11, 14)$ $b_{11} \equiv (8, 9)$ $b_9 \equiv (12, 13)$

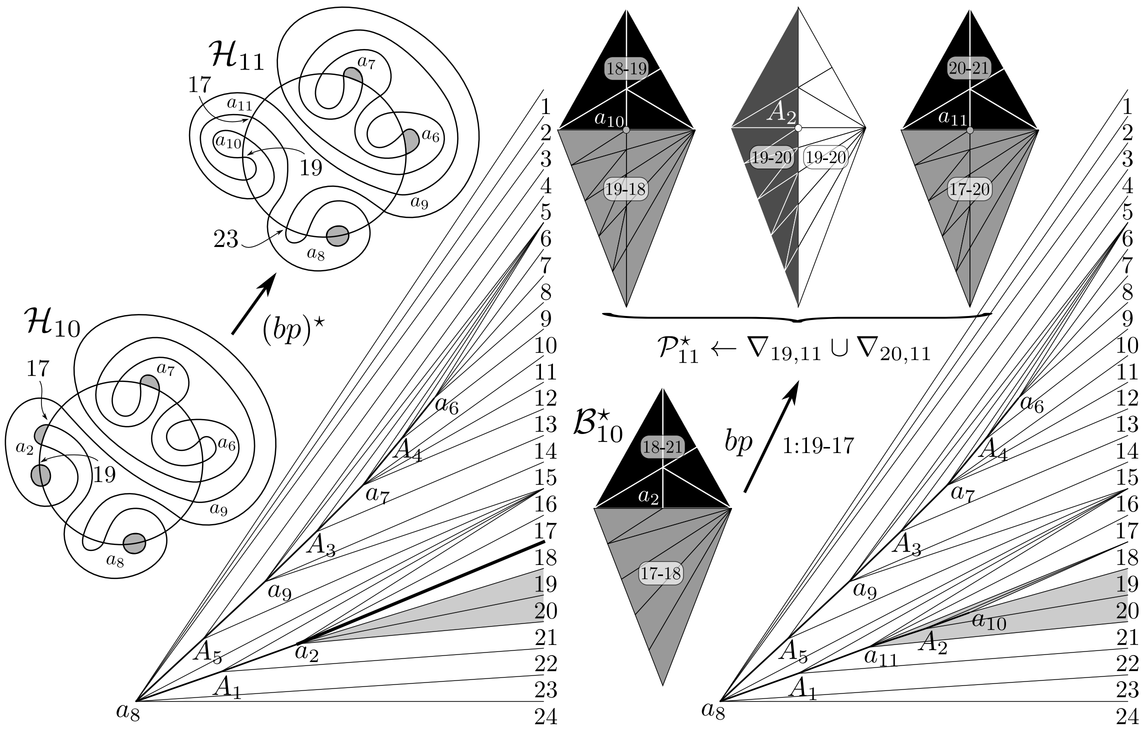

13-gon a_2 is subdivided into a_{10} and a_{11} $a_6 \equiv (9 \downarrow 6)$ $a_7 \equiv (13 \downarrow 10)$ $a_8 \equiv (3 \downarrow 1, 24 \downarrow 22)$
$a_9 \equiv (15, 14, 5, 4)$ $a_{10} \equiv (19, 18)$ $a_{11} \equiv (21, 20, 17, 16)$

Figure 5: The first wbp-move induces another bifurcation on the nervure of a right wing based in b_8. The second wbp-move produces an extension of the nervure of a left wing based on a_2.

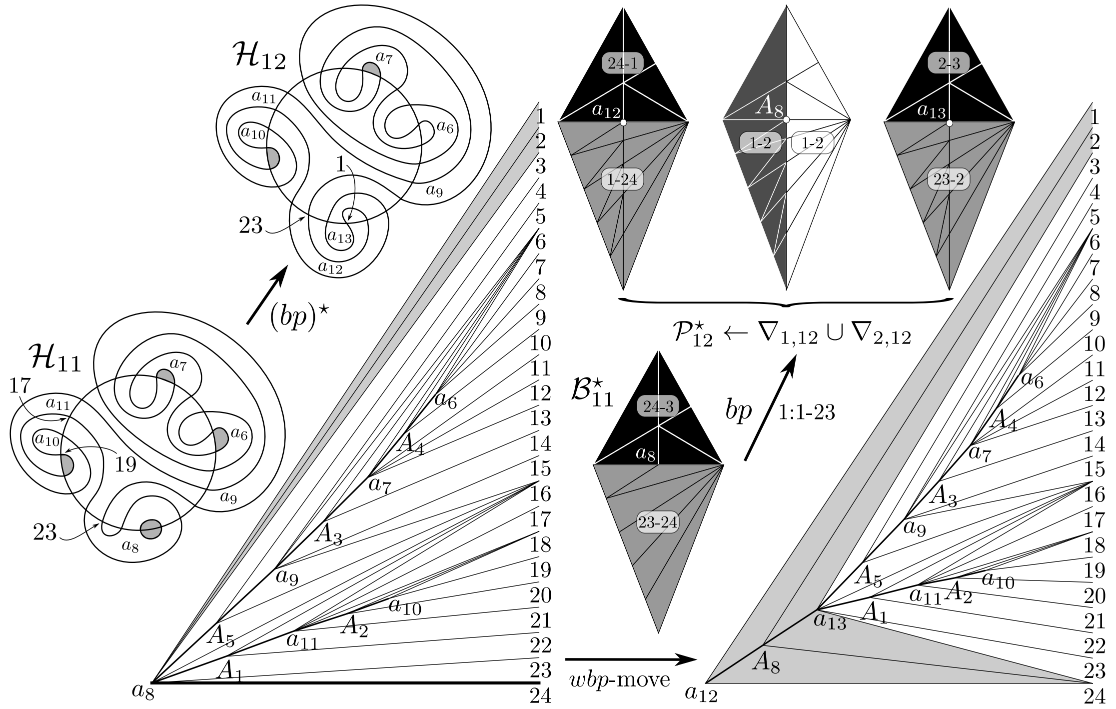

13-gon a_8 is subdivided into a_{12} and a_{13} $a_6 \equiv (9 \downarrow 6)$ $a_7 \equiv (13 \downarrow 10)$ $a_9 \equiv (15, 14, 5, 4)$ $a_{10} \equiv (19, 18)$ $a_{11} \equiv (21, 20, 17, 16)$ $a_{12} \equiv (3, 2, 23, 22)$ $a_{13} \equiv (1, 24)$

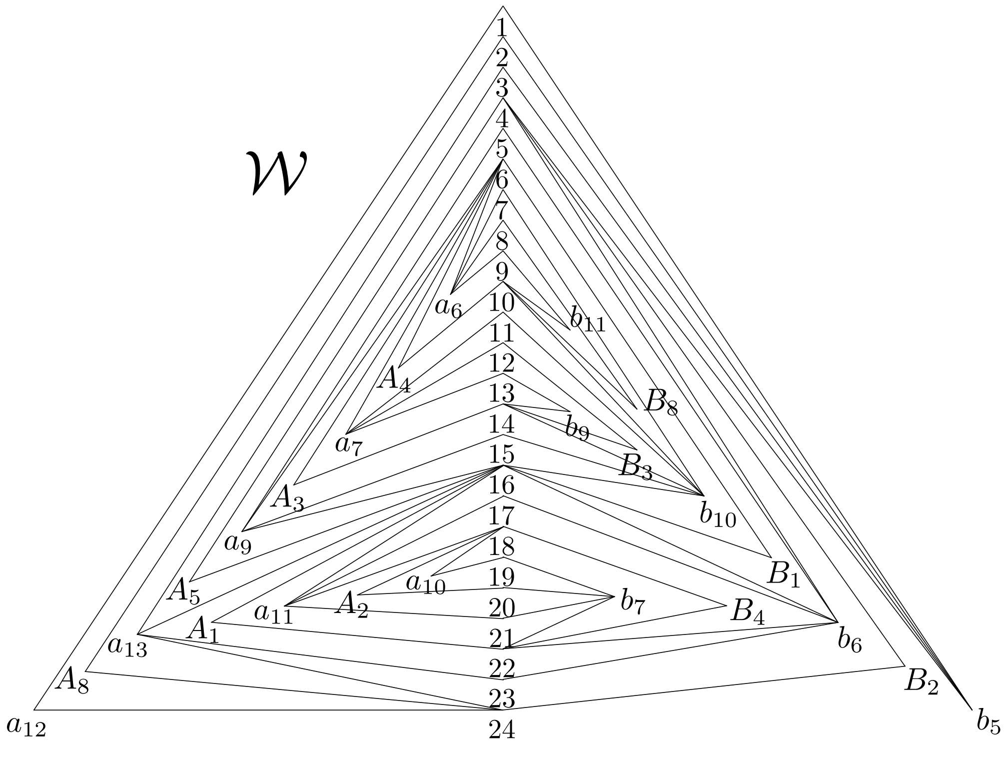

Figure 6: The globally last wbp-move is the extension based at a_8 (correponding to a 13-gon which breaks into two a_{12} and a_{13}). The bottom part of the figure despicts the final pair of wings $\mathcal{W}$. This is the first time that the geometry of the embedding needs to be specified. Up to this point we need only the struts given combinatorially. To obtain the above embedding for $\mathcal{W}$ we have used the deterministic linear algorithm explained in Subection 2.3.

2 Details of the whole construction

2.1 First phase: from a J^2-gem $\mathcal{H}$ to a bloboid $\mathcal{B}$

A k-dipole $\{u, v\}$ involves color i if it if there is an edge of color i linking u to v.

Let H be the J^2-gem formed by the two Jordan curves X and Y. A (X, Y)-*duet* in H is a pair of crossings which are consecutive in X and in Y. A (X, Y)-*trio* in H is, likewise, a triple of crossings that are consecutive in X and in Y.

(2.1) Lemma. *Let H be a J^2-gem with $2n \geq 4$ vertices. Then H has a (X, Y)-trio.*

Proof. By the Jordan theorem H has a (X, Y)-duet D. If $n = 2$ then H has clearly a (X, Y)-trio establishing the basis of the induction. Suppose H has $2n \geq 4$ vertices. It has a (X, Y)-duet D. If D extends to a trio, then we are done. Otherwise slightly deform Y to miss D. The resulting J^2-gem H' has $2n - 2$ crossings and by induction hypothesis H' has a (X, Y)-trio T, which is present in H, establishing the Lemma. □

(2.2) Proposition. *Starting with a J^2-gem $\mathcal{H}$ with $2n$ vertices we can arrive to an n-bloboid $\mathcal{B}$ by means of $n-1$ operations which thickens a 2-dipole involving color 2 into a 3-dipole, where the new edge is of color 0 or color 1, producing a sequence of J^2B-gems each inducing $\mathbb{S}^3$,*

$$(\mathcal{H} = \mathcal{H}_n, \mathcal{H}_{n-1}, \ldots, \mathcal{H}_2, \mathcal{H}_1 = \mathcal{B}).$$

Proof. The proof is by backward induction. For $\ell = n$ we have $\mathcal{H}_n = \mathcal{H}$ and so it is a J^2B-gem, establishing the basis of the induction. Assume that $\mathcal{H}_\ell$ is a J^2B-gem. For $\ell > 1$, let $\mathcal{H}'_\ell$ denote $\mathcal{H}_\ell$ after cancelling the blobs. By Lemma 2.1 $\mathcal{H}'_\ell$ has a (X, Y)-trio (x, y, z). Thus y is incident to two 2-dipoles. One of these dipoles, call it D, involves color 2, the other involves color 3. Take the one involving color 2, name it D. Put back the blobs over the edges of color 3. So, D is present in $\mathcal{H}_\ell$. The colors involved in D are 0 and 2 or 1 and 2. In the first case we use color 1 to thicken D and in the second we use color 0 for the same purpose. This defines the J^2B-gem $\mathcal{H}_{\ell-1}$, which establishes the inductive step. In face of Proposition 1.1 and from the fact that thickening dipoles on gems produce gems inducing the same manifold, every member of the sequence induces $\mathbb{S}^3$. □

2.2 Second phase: colored abstract complexes, their wings, nervures

The second phase starts with an easy task, namely to define the dual of the bloboid, named $\mathcal{H}^\star_1$. We get this first term in an embedded form. The others $\mathcal{H}^\star_2$, ..., $\mathcal{H}^\star_n$, are, at this stage, obtained by slight modifications of the antecessor, but only in an abstract compinatorial way. In doing so we get the minimum level of refinement in the PL2-faces required, so that latter, the levels are sufficient for a geometric PL-embedding in $\mathbb{R}^3$ which we seek.

2.2.1 Primal and dual correspondence between the gem and the colored complex

There is a simple topological interpretation between primal and dual complexes, given in [8] pages 38, 39. Let us take a look at this interpretation in our context. This will help to understand the PL-embedding $\mathcal{H}^\star_m$. In what follows the k in PLk-face means the dimension $k \in \{0, 1, 2, 3\}$ of the PL-face.

i. a vertex v in $G \rightleftharpoons$ a solid PL-tetrahedron or PL3-face, denoted by ∇_v in the dual of the gem whose PL0-faces are labelled z_0, z_1, z_2 e z_3^v; in this work, it is enough to work with the boundary of a PL3-face; this is topologically a sphere $\mathbb{S}^2$ with four PL2-faces one of each color; the 3-simplices forming a PL3-face need not be explicitly specified;

ii. an i colored edge e_i in $G \rightleftharpoons$ a set of i-colored 2-simplices defining a PL2$_i$-face in the dual of the gem;

iii. a bigon B_{ij} using the colors i, j in $G \rightleftharpoons$ a set of 1-simplices b_{ij} in $\mathcal{H}_n^\star$ defining a PL1$_{ij}$-face;

iv. an $\bar{i}$-residue V_i in $G \rightleftharpoons$ a 0-simplex in $\mathcal{H}_n^\star$ defining a PL0$_i$-face.

2.2.2 Defining $\mathcal{H}_1^\star$ and the colored abstract PL-complexes: $\mathcal{H}_2^\star$, ..., $\mathcal{H}_n^\star$

We define the combinatorial 2-dimensional PL complex $\mathcal{H}_1^\star$ as follows.

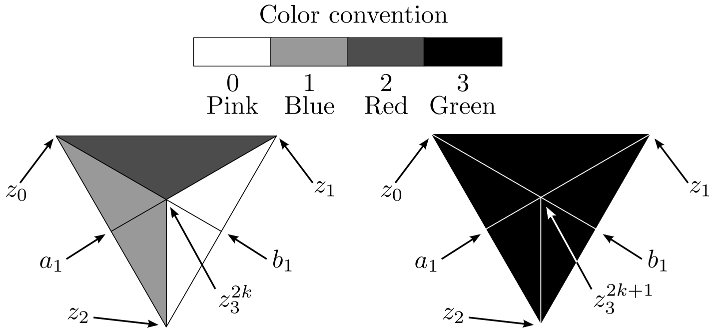

Figure 7: PL2-faces of $\mathcal{H}_1^\star$: the figure is an abreviation of a stack of tetrahedra, where $k = 0, 1, \ldots, n-1$. The 0-simplices z_3^j are defined as $z_3^j = (0, 0, 2n - j)$, $1 \leq j \leq 2n$. For even $j = 2k$, there are five simplices incident to z_3^j: two 0-colored, two 1-colored and 1 2-colored. For odd $j = 2k + 1$, the five 2-simplices incident to z_3^j are all 3-colored. The 0-simplices z_0, z_1 and z_2 are positioned in clockwise order as the vertices of an equilateral triangle of side 1 in the xy-plane so that z_0z_1 is parallel to the x-axis and the center of the triangle coincides with the origin of an $\mathbb{R}^3$-cartesian system. The 0-simplex a_1 is $\frac{z_0+z_2}{2}$. The 0-simplex b_1 is $\frac{z_2+z_1}{2}$. Note that, in general, the PL3-faces are given by their boundary. We never use 3-simplices explicitly to triangulate the PL3-faces. From our construction, however, it will be clear that this is possible to achieve without spurious intersections among the 3-simplices.

We detail the connection of the J^2-gem and its dual. In particular we use the unique 23-gons of it to provide labels $1, 2, \ldots, 2n$ in the cyclic order of the 23-gon. This labellings correpond to PL3-faces of the $\mathcal{H}_1^\star$ and will be maintained for the PL3-faces of the whole remaining sequence $\mathcal{H}_2^\star$, ..., $\mathcal{H}_n^\star$. This invariance is a dual manifestation of the fact that in the thickening of dipoles the labels of the vertices preserved. Suppose u is an odd vertex of the J^2-gem, $u' = u - 1$, $v = u + 1$ and $v' = v + 1$. The dual of a $\overline{3}$-residue is z_3^j where j is even. When j is odd, then z_3^j is a 0-simplex in the middle of a PL2$_3$-face, incident to five 2-simplices of color 3. The dual of the 03-gon is the PL1-face formed by the pair of 1-simplices z_1b_1 and b_1z_2. The dual of the 13-gon is the PL1-face formed by the pair of 1-simplices z_0a_1 and a_1z_2. The dual of the 23-gon is the PL1-face formed by the 1-simplex z_0z_1. The dual of the 01-gon relative to vertices u and v is the 1-simplex $z_2z_3^v$. The dual of the 02-gon relative to vertices u and v is the 1-simplex $z_1z_3^v$. The dual of the 12-gon relative to vertices u and v is the 1-simplex $z_0 z_3^v$. The dual of a 3-colored edge $u'u$ is the image of $\text{PL}2_3$-face with odd index u in the vertices. The dual of an i-colored edge uv with $i \in \{0, 1, 2\}$ is the $\text{PL}2_i$-face with even index v.

2.2.3 Primal and dual *bp*-moves

Before presenting $\mathcal{H}_m^\star$, $1 < m \leq n$, and its embeddings, we need to understand the dual of the $(pb)^\star$-move and its inverse. In the primal, to apply a $(pb)^\star$-move, we need a blob and a 0- or 1-colored edge. The dual of this pair is the *balloon:* the *balloon's head* is the dual of the blob; the *balloon's tail* is the dual of the i-edge. To make it easier to understand, the $(pb)^\star$-move can be factorable into a 3-dipole move followed by a 2-dipole move, so in the dual, it is a smashing of the head of the balloon followed by the pillow move described in the book [8], page 39. This composite move is the *balloon-pillow move* or *bp-move.* Restricting our basic change in the colored 2-complex to *bp*-moves we have nice theoretical properties which are responsible for avoiding an exponential proccess.

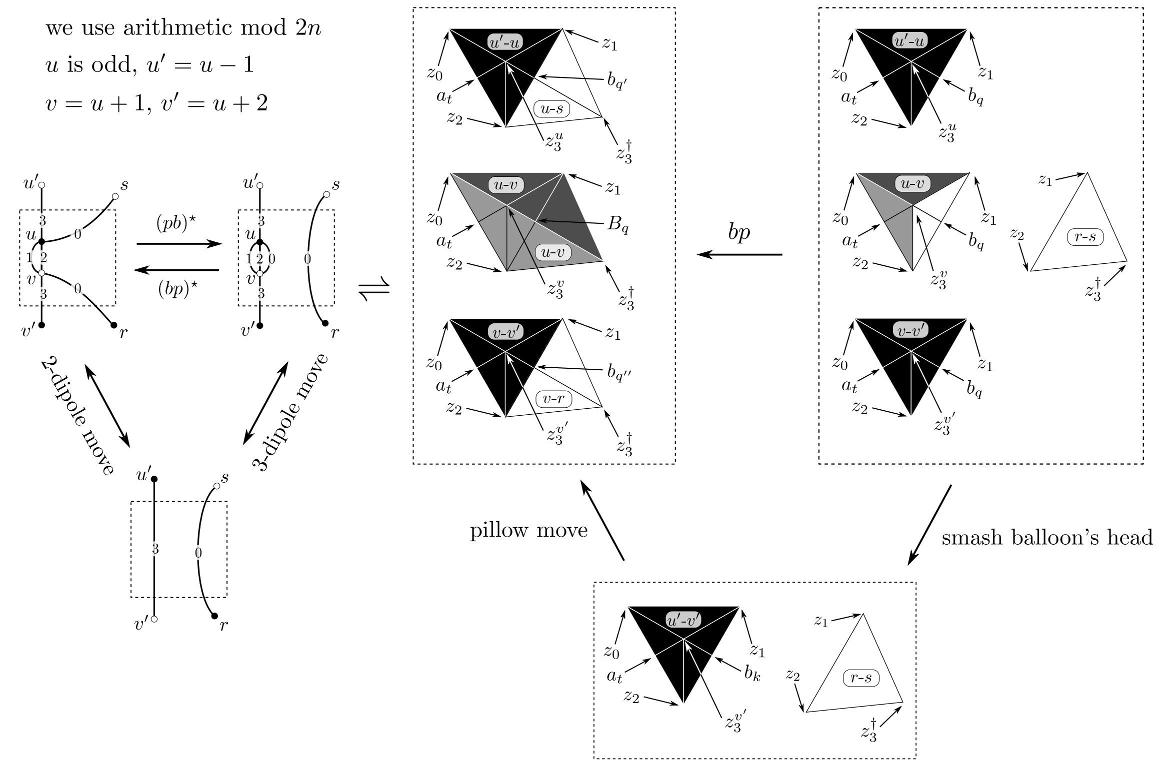

Figure 8: Primal and dual *bp*-moves: in what follows we describe the *bp*-move assuming that the balloon's tail is 0-colored using a generic balloon's tail, of which we just draw the contour. The other case, color 1, is similar. (1) if the image of v_5^u and v_5^v is b_q, create two 0-simplices $b_{q'}$ and $b_{q''}$, define the images of v_5^u and $v_5^{v'}$ as $b_{q'}$ and $b_{q''}$ and change the label of the image of v_5^v from b_q to B_q; (2) make two copies of the $\text{PL}2_0$-face, if necessary, refine each, from the middle vertex of the segment $z_2 z_1$ to the third vertex $z_3^\dagger$, where $\dagger = j$, for an adequate height j; (3) change the colors of the medial layer of the pillow as specified by the dual structure, namely by the current J^2B-gem.

2.2.4 Types of PL2-faces

(2.3) Proposition. *Each PL2-face of the combinatorial simplicial complex $\mathcal{H}^\star_m$, $1 \le m \le n$, is isomorphic to one in the* set of types of triangulations

$$\{G, P_{2k-1}, P'_{2k-1}, B_{2k-1}, B'_{2k-1}, R^b_{2k-1}, R^p_{2k-1} \mid k \in \mathbb{N}\},$$

described in Fig. 9, where the index means the number of edges indicated and is called the rank of the type. *Moreover, the PL2-faces that appear, as duals of the gem edges, have the minimum number of 2-simplices.*

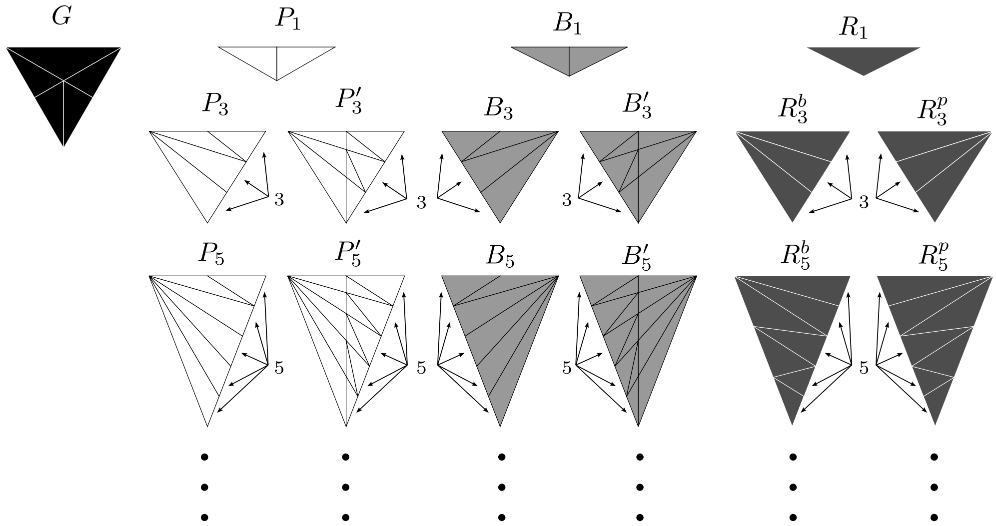

Figure 9: All kinds of PL2-faces that we use: the choice of the letters P, B, R, G comes from the colors $0 = (P)ink$, $1 = (B)lue$, $2 = (R)ed$ and $3 = (G)reen$. Define R^b_{2k-1} as the $\mathrm{PL2}_2$-face which is inside the pillow neighboring a $\mathrm{PL2}_1$-face. Similarly R^p_{2k-1} is a $\mathrm{PL2}_2$-face which is inside the pillow neighboring a $\mathrm{PL2}_0$-face.These PL2-faces are for now abstract combinatorial triangulations that have the correct level of refinement so as to become PL-embedded into $\mathbb{R}^3$.

Proof. We need to fix a notation for the head of the balloon. Instead of drawing all the PL2-faces of the head, we just draw one $\mathrm{PL2}_3$-face and put a label u'-v'. If the balloon's tail, is of type P_1, by applying a bp-move we can see at Fig. 10 that we get a $\mathrm{PL2}_1$-face of type B_3 and a

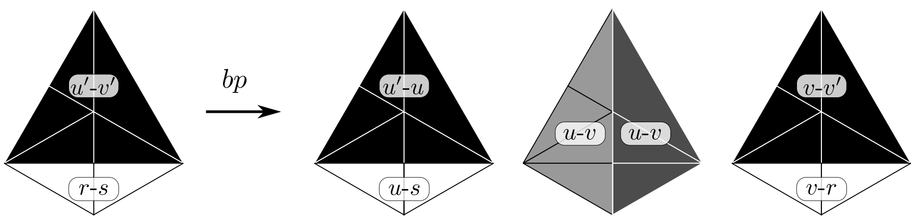

Figure 10: A bp-move with the balloon's tail of type P_1.

$\mathrm{PL2}_2$-face of type R^b_3. The others PL2-faces are already known. If the balloon's tail, is of type

B_3, by applying a bp-move, we need to refine the tail and the copies, otherwise we would not be able to build a pillow because some 2-simplices would be collapsed, so we get two PL2_1-faces of type B'_3, one PL2_0-face of type P_5 and a PL2_2-face R^p_5. The others PL2-faces are already known.

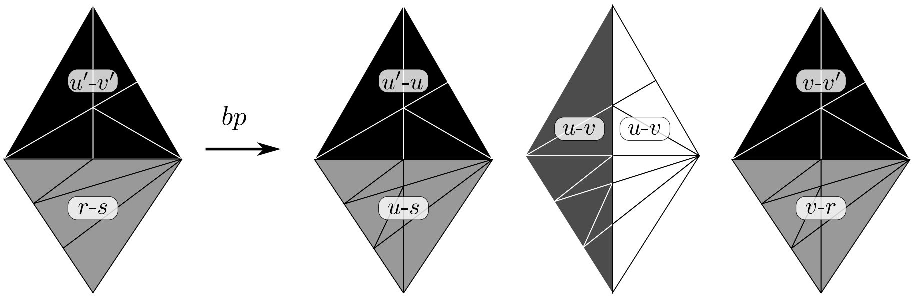

Figure 11: A bp-move with the balloon's tail of type B_3.

In what follows given $X \in \{P'_{2k-1}, B'_{2k-1}\}$ denote by $\overline{X}$ the copy of X which is a PL2-face of the PL-tetrahedra whose PL2_3-face is below the similar PL2_3-face of the other PL-tetrahedra which completes the pillow in focus. In face of these conventions, if balloon's tail is of type

- P_{2k-1}, then by applying a bp-move, we get types $P'_{2k-1}, \widehat{P}'_{2k-1}, B_{2k+1}, R^b_{2k-1}$
- P'_{2k-1}, then by applying a bp-move, we get types $P_{2k-1}, B_{2k+1}, R^b_{2k-1}$
- B_{2k-1}, then by applying a bp-move, we get types $B'_{2k-1}, \widehat{B}'_{2k-1}, P_{2k+1}, R^p_{2k-1}$
- B'_{2k-1}, then by applying a bp-move, we get types $B_{2k-1}, P_{2k+1}, R^p_{2k-1}$

The necessary increasing in the ranks of the types of faces shows that the rank of each face is at least the one obtained. It may cause a surprise the fact that these ranks are enough to make the PL-embedding geometric into $\mathbb{R}^3$. □

It is whorthwhile to mention, in view of the above proof, that each PL2-face is refined at most one time. So, if X is a type of PL2-face, X' is its refinement, then $X'' = X'$. This idempotency is a crucial property inhibiting the exponentiality of our algorithm and enables a quadratic bound.

2.2.5 Quadratic bounds on the number of simplices

(2.4) Corollary. *The quadratic expressions*

$$3n^2 - 5n + 9, \quad 11n^2 - 17n + 21, \quad 8n^2 - 10n + 12$$

are upper bounds for the numbers of 0-simplices, 1-simplices and 2-simplices of the colored 2-complex $\mathcal{H}^\star_n$ induced by a resoluble gem G with $2n$ vertices.

Proof. We prove the first bound, on 0-simplices; the other are similar: in the worse case, the increase of simplices is a linear function on the rank of the current PL2-face, and to get the final number we sum an arithmetic progreesion.

We detail the strategy for 0-simplexes. Note that $\mathcal{H}^\star_1$ has exactly z_0, z_1, z_2, a_1, b_1 and $z^j_3, j \in \{1, \ldots, 2n\}$ as 0-simplices, which is $2n + 5$ 0-simplices. In the first step, the balloon's tail has to be of type P_1 or B_1, so by applying a *bp*-move, we get two new 0-simplices. In second step, the worst case is when the balloon's tail is of type P_3 or B_3, generated by last *bp*-move, so we add $6 \times 1 + 2 = 8$ to the number of 0-simplices in the upper bound. In step k we note that the worst case is when we use the greatest ranked PL2-face generated by last *bp*-move, therefore the balloon's tail has to be of type P_{2k-1} or B_{2k-1} and we add $6 \cdot (k-1) + 2$ 0-simplices. By adding the number of 0-simplices created by *bp*-moves from step 1 until step k we get $3k^2 - k$ 0-simplices. Since the number of steps is $n-1$, and we have at the begining $2n+5$ 0-simplices, we have that $3n^2 - 5n + 9$ is an upper bound for the number of 0-simplices. □

2.2.6 Detailing the combinatorics of the wings, nervures and struts

An embedding of a graph into an oriented surface is combinatorially encoded as a *rotation at the vertices* or simply a *rotation*. A rotation is the set of cyclic orderings of the edges around the vertices (induced by the surface) so that each edge appears exactly twice, one with each orientation. We encode the struts as rotations. Only the last one needs to be dealt with geometrically.

At some point in our research it became evident that what was needed to obtain the embedded PL-complex $\mathcal{H}_n^\star$ was a proper embedding into $\mathbb{R}^3$ of two special sequences of 0-simplices $\mathcal{A} = (a'_1, a'_2, \ldots, a'_f)$ and $\mathcal{B} = (b'_1, b'_2, \ldots, b'_g)$, where $f+g = 2n$. Each $a'_i \in \{a_i, A_i\}$ and each $b'_i \in \{b_i, B_i\}$. This terminology for the 0-simplices is obtained recursively and detailed shortly in this section. For now we just say that all other 0-simplices not in $\mathcal{A} \cup \mathcal{B}$ of the colored complexes $\mathcal{H}_m^\star$ are obtained by bisections of segments linking previously defined points. It came as a surprise to discover that the apparently difficult 3D problem of positioning $\mathcal{A} \cup \mathcal{B}$ could be reformulated as a plane problem with an easy solution, via a linear unique solution algorithm. That is the role of the wings, nervures and struts associated to the colored complexes.

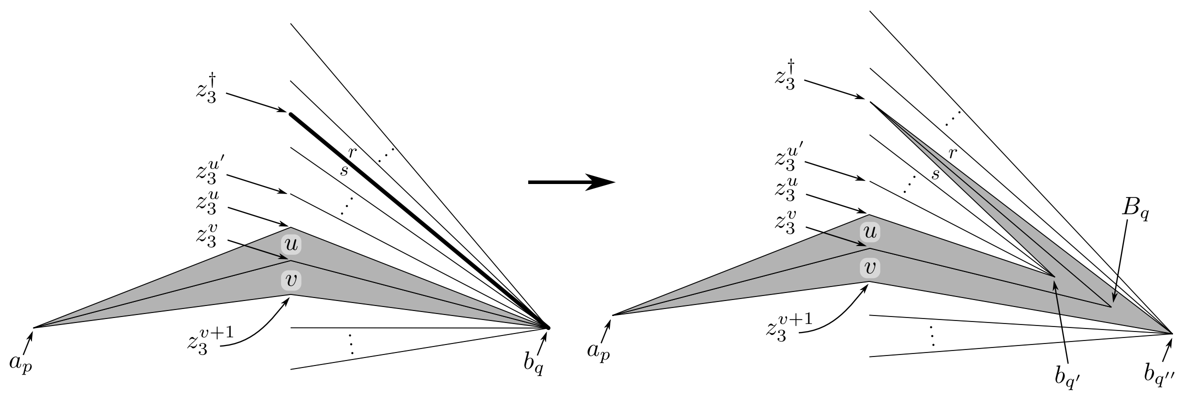

Figure 12: Generic *wbp*-move: balloon's head section is painted in gray, and the part of balloon's tail that is intersecting the appropriate semi-plane (Π'') is depicted as a *thick edge*.

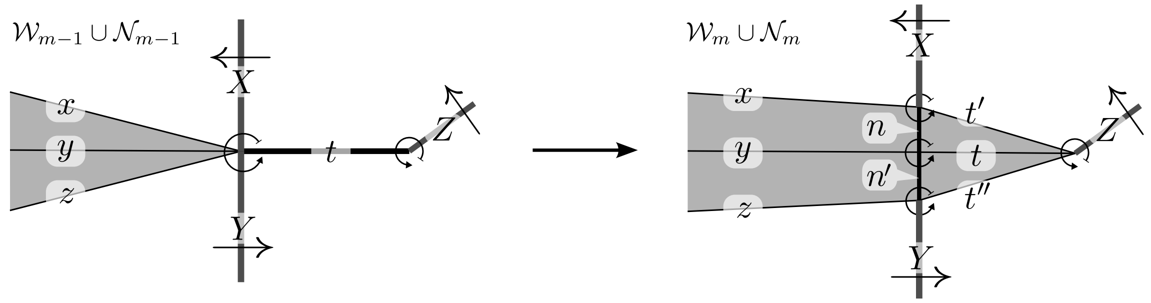

Figure 13: The effect of the general wbp-move in the combinatorial strut: the *star* of a vertex of a graph embedded in an onrientable surface (in our case the plane) is the counterclockwise cyclic sequence of edges incident to the vertex (such an ordering is induced by the surface). The set of stars is called a *rotation* and has the characterizing property that each edge appears twice. The general case of changing rotation when going from $\mathcal{W}_{m-1} \cup \mathcal{N}_{m-1}$ to $\mathcal{W}_m \cup \mathcal{N}_m$ is depicted above: labels X, Y, Z stand for arbitrary (maybe empty) sequences of edges; the vertex $XxyzYt$ breaks into three $Xxnt'$, $nyn't$ and $n'zYt''$ and the vertex Zt changes into $Zt'tt''$. Two new vertices and four new edges are created. Two of these edges (n and n') are in the nervure $\mathcal{N}_m$ and the other two (t' and t'') are in the wing $\mathcal{W}_m$. The new rotation completely specifies the topological embedding of $\mathcal{W}_m \cup \mathcal{N}_m$.

(2.5) Algorithm (Obtaining the rotations for the struts, arriving to $\mathcal{S}_n$). *BEGIN:* $i = 1$; $\mathcal{W}_i = \mathcal{W}'_i \cup \mathcal{W}''_i$ *is formed by* $2n$*-edges linking* a_1 *to* Z *and* $2n$ *edges linking* b_1 *to* Z*; we also have* $\mathcal{N}_1 = \varnothing$*; REPEAT:* $i \leftarrow i + 1$*; there are two cases, according to the color of the edges which are flipped in the associated thinning of a blob is 1 or 0; in the first case the strut that changes is the left one (while* $\mathcal{S}''_i = \mathcal{S}''_{i-1}$*), in the other case it is the right strut that changes (while* $\mathcal{S}'_i = \mathcal{S}'_{i-1}$*); perform the appropriate wbp-move creating two new vertices* $a_{2\ell}, a_{2\ell+1}$ *in the first case or* $b_{2\ell}, b_{2\ell+1}$ *in the second (*$2\ell - 1$ *is the last index of* $\mathcal{A}$ *or of* $\mathcal{B}$*); let* a_q *(resp.* b_q*) denote the 13-gon (resp. the 03-gon) which is being subdivided; then we relabel* a_q *as* A_q *(resp.* b_q *as* B_q*); these capital letter labeled 0-simplices no longer correspond to bigons, while bigon* a_q *(resp* b_q*) has been subdivided into* $a_{2\ell}, a_{2\ell+1}$ *(resp.* $b_{2\ell}, b_{2\ell+1}$*); also 2 new edges are added when going from* $\mathcal{S}_{m-1}$ *to* $\mathcal{S}_m$ *according to the rotation changing of Fig. 13; UNTIL* $i = n$*; Output* $\mathcal{S}_n$*; END.*

It is easy to verify that the above algorithm is linear in n. Now we need to make $\mathcal{S}'_n$ rectilinearly embedded into Π' and $\mathcal{S}''_n$ rectilinearly embedded into Π''. This is provided in the next subsection.

2.3 Third phase: a rectilinear PL-embedding for $\mathcal{S}_n$ and its induced diamond complex $\mathcal{H}_1^\diamond$, by a cone construction

A graph is *rectilinearly embedded into a plane* if the images of their edges are straight line segments. We will find by a linear algorithm a rectilinear embedding for $\mathcal{S}_n$. We do it in the plane and lift it to space by two simple rotations to position $\mathcal{S}'_n$ in Π' and $\mathcal{S}''_n$ in Π''.

(2.6) Lemma. *The number of edges of* $\mathcal{S}_n$ *is* $8n - 4$.

Proof. The number of edges of $\mathcal{S}_1$ is $4n$. At each of the $n - 1$ bp-moves we add 4 new edges. □

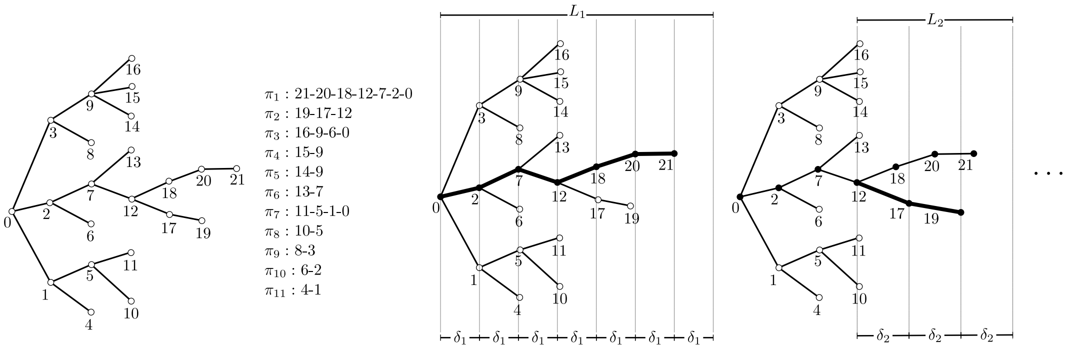

Figure 14: Algorithm to find the x-coordinates of the vertices of the left nervure $\mathcal{N}'$ (the right nervure $\mathcal{N}''$ is similar). BEGIN: find the BFS-number ([2]) of vertices of the tree $\mathcal{N}'$ with root vertex being the leftmost one of $\mathcal{N}'$. Let the vertices be labeled by its BFS-number. In the algorithm, we use a partition of the edges of $\mathcal{N}'$ into paths; make all vertices except the root unused; $i = 0$; make the path partition empty; REPEAT: $i \leftarrow i + 1$; take the ancestor path π_i starting with the highest BFS-numbered vertex not yet used and finishing at the first used vertex; put the sequence of vertices of π_i defining a new member of the edge-path partition; declare all the vertices in π_i as used; let δ_i be L_i/λ_i, where L_i is the x-distance from the first and last vertices of π_i and λ_i is the number of vertices in π_i; let δ_i be the x-distance between consecutive vertices of π_i (note that the x-coordinate of the last vertex of π_i has been already defined and so the x-coordinates of the all the vertices of π_i becomes fixed, never to change); UNTIL all vertices are used; END.

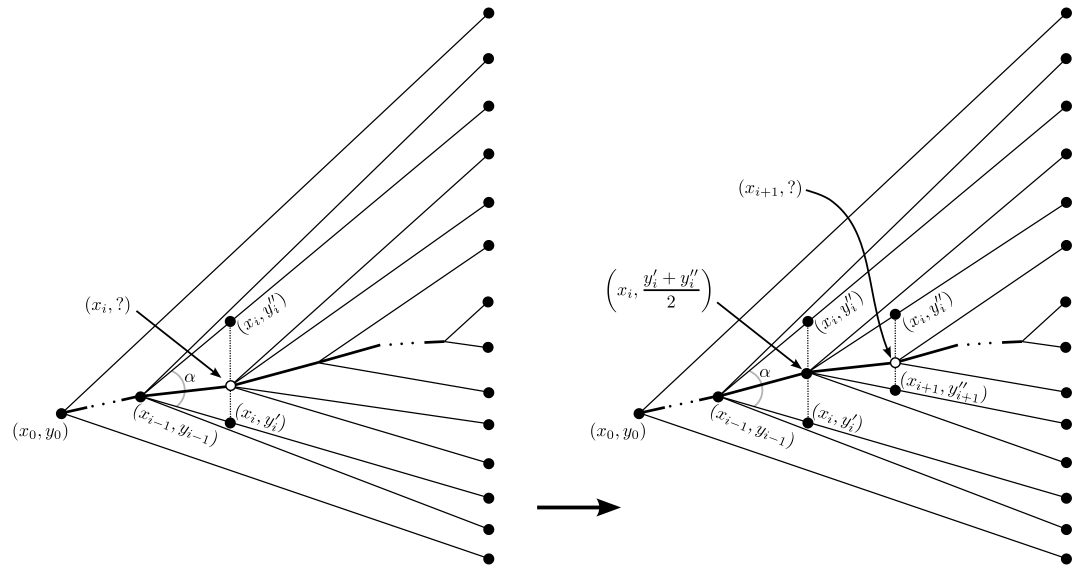

Figure 15: A linear algorithm for rectilinearly embedding $\mathcal{W}'$, that is, the last left wing (the right side of the last wing $\mathcal{W}''$ is similar). BEGIN: by using the Algorithm of Fig. 14 we have already the x-coordinates of all the vertices of $\mathcal{W}'$. Let $\gamma_1, \gamma_2, \ldots \gamma_k$ be the sequence of inverses of the paths π_i's, obtained in the algorithm of Fig. 14; let y_1^1 be the y-coordinate of the first vertex of γ_1; $y_1^1 \leftarrow 0$; $i \leftarrow 0$; REPEAT: $i \leftarrow i+1$; $j \leftarrow 0$; REPEAT: $j \leftarrow j+1$; let e_{ij} be the edge in the nervure incident to γ_i^j (the j-th vertex in the path γ_i) and γ_i^{j-1}; let e'_{ij} be the edge which succeeds e_{ij} and e''_{ij} be the edge that preceeds it in the counterclockwise rotation of vertex γ_i^{j-1}; note that the other ends of e'_{ij} and e''_{ij} are z_3^p and z_3^q for some $p < q$; (Obs: in the case of γ_1^1 it might happen that e''_{11} does not exist; in this case define e''_{11} as a virtual edge that links γ_1^1 to z_3^{2n}, where $2n$ is the number of vertices of the J^2-gem); let v be the intersection of the line $x = x_i^j$ and the edge e'_{ij}; let w be the intersection of the line $x = x_i^j$ and the edge e''_{ij}; $y_i^j \leftarrow (v+w)/2$; UNTIL $j =$ length of γ_i; UNTIL $i = k$; END.

We apply the algorithms of the previous two figures to obtain a rectilinear embedding of $\mathcal{W}$ in linear time. The connection between $\mathcal{W}$, $\mathcal{W}_1^\diamond$ and $\mathcal{H}_1^\diamond$ is explained in Figure 16.

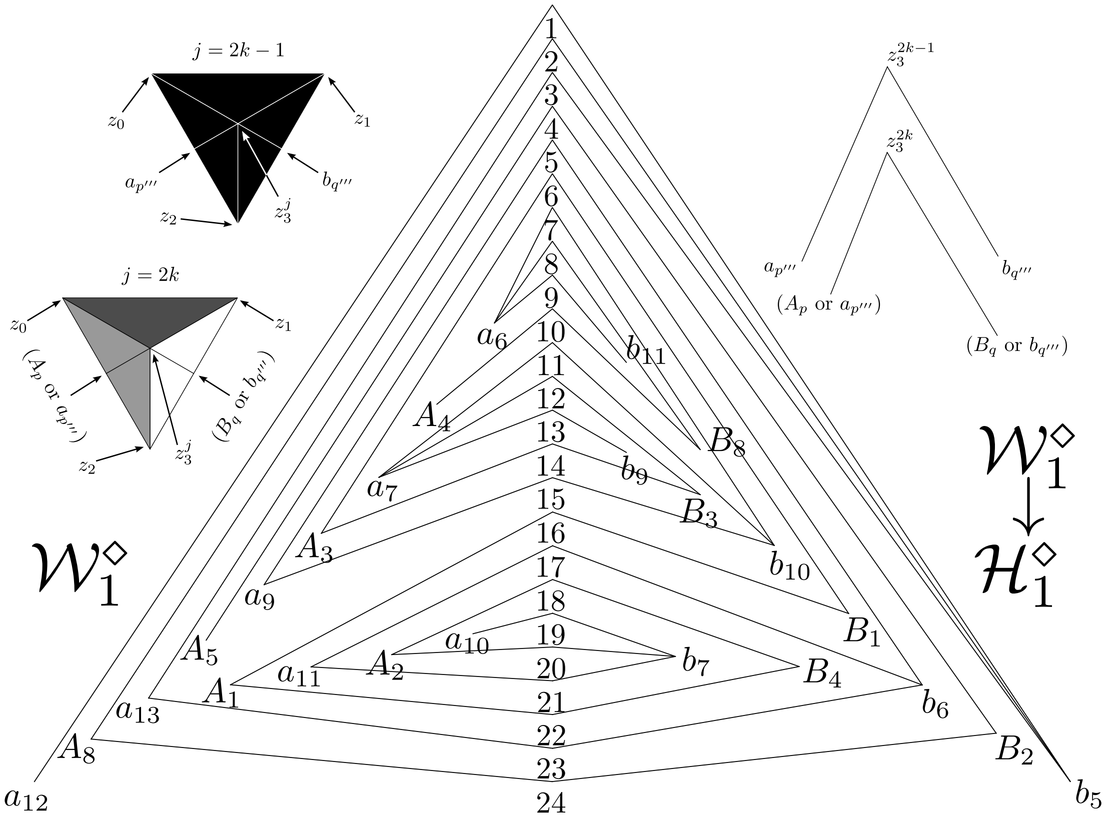

Figure 16: To get $\mathcal{W}_1^\diamond = \mathcal{W}_1^{\diamond'} \cup \mathcal{W}_1^{\diamond''}$ from $\mathcal{W}$ remove all but two straight line segments emanating from z_3^k, one in each side. The two segments that survive are the ones finishing at the smallest index upper case A_p (when there is a choice) and the smallest indexed upper case B_q (when there is a choice). Let $\{x\} \cup Y \subseteq \mathbb{R}^N$, for $1 \leq N \in \mathbb{N}$. The *cone* [12] with vertex x and base Y, denoted $x * Y \subseteq \mathbb{R}^N$, is the union of Y with all line segments which link x to $y \in Y$. The passage $\mathcal{W}_1^\diamond \to \mathcal{H}_1^\diamond$ is straighforward by a cone algorithm: for each $e' \in \mathcal{W}_1^{\diamond'}$ add the two 2-simplices $z_0 * e'$ and $z_2 * e'$ to $\mathcal{H}_1^\diamond$; for each $e'' \in \mathcal{W}_1^{\diamond''}$ add the two 2-simplices $z_1 * e''$ and $z_2 * e''$ to $\mathcal{H}_1^\diamond$. To complete $\mathcal{H}_1^\diamond$ add the 2-simplices $\{z_3^j z_1 z_0 \mid j = 1, \ldots, 2n\}$.

2.4 Fourth phase: filling the pillows, to obtain the PL-embedding of $\mathcal{H}^\star$ we seek: $\mathcal{H}_1^\diamond, \mathcal{H}_2^\diamond, \ldots \mathcal{H}_{n-1}^\diamond, \mathcal{H}_n^\diamond = \mathcal{H}^\star$

We start the fourth phase with $\mathcal{W}_1^\diamond$ and $\mathcal{H}_1^\diamond$, which is defined in Fig. 16.

(2.7) Proposition. *If $\mathcal{W}_1^\diamond$ is embedded rectilinearly in $\Pi' \cup \Pi''$, then it can be extended to an embedding of $\mathcal{H}_1^\diamond$ into $\mathbb{R}^3$, via the cone construction.*

Proof. Straighforward from the simple geometry of the situation. See Fig. 16. □

Let $\mathcal{L}_{i+1}^\star$ be a subset of the pillow $\mathcal{P}_{i+1}^\star$, formed by the part that comes from the tail of the balloon after the i-th *bp*-move is applied, see Fig. 17.

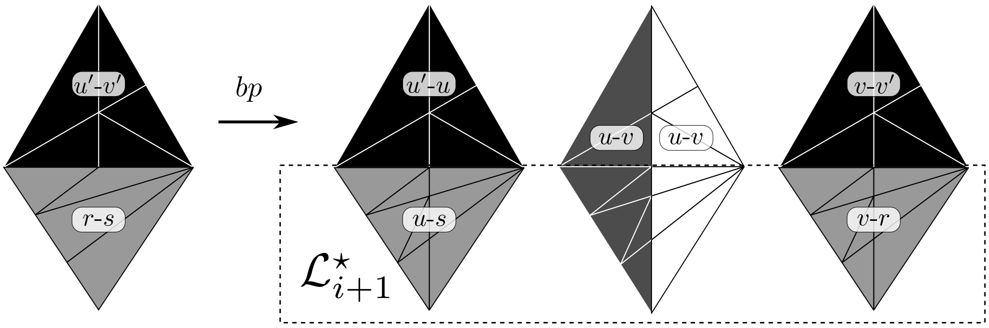

Figure 17: The set $\mathcal{L}^\star_{i+1}$'s: at each step of Theorem 2.8 we embed a set $\mathcal{L}^\star_{i+1}$, $i = 0, \dots n-1$ of 2-simplices. These sets are the complemetary parts of the PL2-faces already in $\mathcal{H}^\diamond_1$ after a change of colours in the medial layer. The process of replacing the combinatorial tail of a balloon by the corresponding trio of embedded PL2-faces in the pillow is denominated *the blowing up of the balloon's tail*.

(2.8) Theorem. *There is an $O(n)$-algorithm for blowing up a single balloon's tail. Thus finding $\mathcal{H}^\star_n$ take, $O(n^2)$ steps.*

Proof. $\mathcal{H}^\diamond_{i+1}$ is the union of $\mathcal{H}^\diamond_i$ with $\mathcal{L}^\star_{i+1}$ and an ϵ-*change* in some PL3-faces, if the rank of the type of balloon's tail of the i-th bp-move has rank greater than 1 (we call ϵ-change because this change is small, as described below). At the same time we update the colors of the middle layer to match the colors of the i-th pillow in the sequence of bp-moves.

Now we describe how to embed each kind of $\mathcal{L}^\star_i$ (explaining how to ϵ-change some PL3-faces, to get space for $E\mathcal{L}^\star_i$).

If the balloon's tail is of type P_1 (the case B_1 is analogous). Make two copies of P_1, resulting in three P_1, but change the color of the one which will be in the middle, and define the 0-simplices like in Fig. 18.

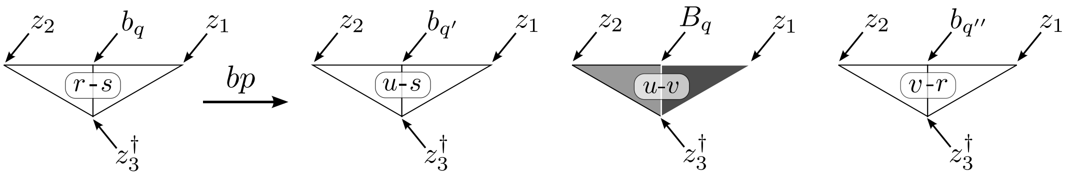

Figure 18: Embedding the part of the pillow corresponding to the tail of the balloon: case P_1 of the tail.

If the balloon's tail is of type B_i, $i > 1$ (the case P_i is analogous). Make two copies of B_i, refine the copies and the original, resulting in three B'_i, but change the color of the one which will be in the middle, and define the 0-simplices like in Fig. 19.

The images χ_j we already know from previous bp-move, now we need to define all the images α_j, β_j and γ_j. Let β_j be $\frac{z_2+\chi_{j+1}}{2}$ for each $j = 1, \dots, i$. As the images α_j and γ_j can be defined in analogus way, we just explain how to define each α_j. We know that each α_j is in the PL3-face ∇_r. To define each α_j we need to reduce the PL3-face ∇_r in order to get enough space for the PL2-faces of color 0 and 2 of the PL3-faces ∇_u and ∇_v. Consider the PL3-face ∇_r, each β_j is already defined, so define each ζ_j as $\frac{z_2+\omega_{j+1}}{2}$, where ω_k is previously defined, see Fig. 20. Define α_j as $\frac{\zeta_j+\beta_j}{2}$.

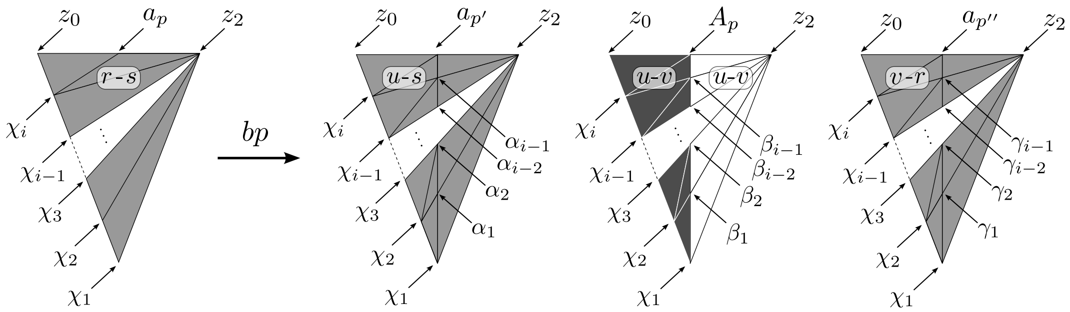

Figure 19: Embedding the part of the pillow corresponding to the tail of the balloon: case B_i of the tail.

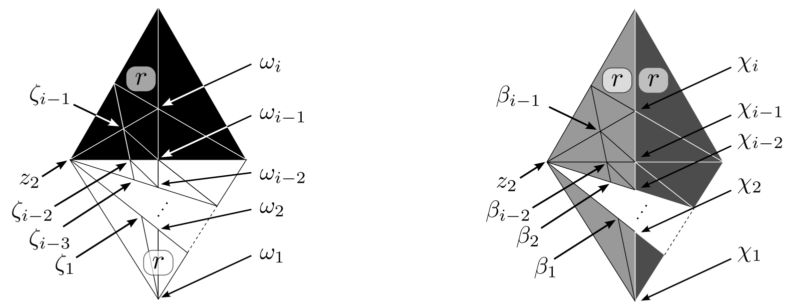

Figure 20: Using the PL3-face corresponding to r to define the α_j as $\frac{\zeta_j+\beta_j}{2}$.

The last case is when balloon's tail is refined, that means it is of type P_i' or B_i', $i > 1$. We treat the case B_i', see Fig. 21. All the 0-simplices β_j are already defined, we need to define each α_j and each γ_j. Observe that here $r \neq s-1$ and the definitions of α_j and γ_j are not analogous.

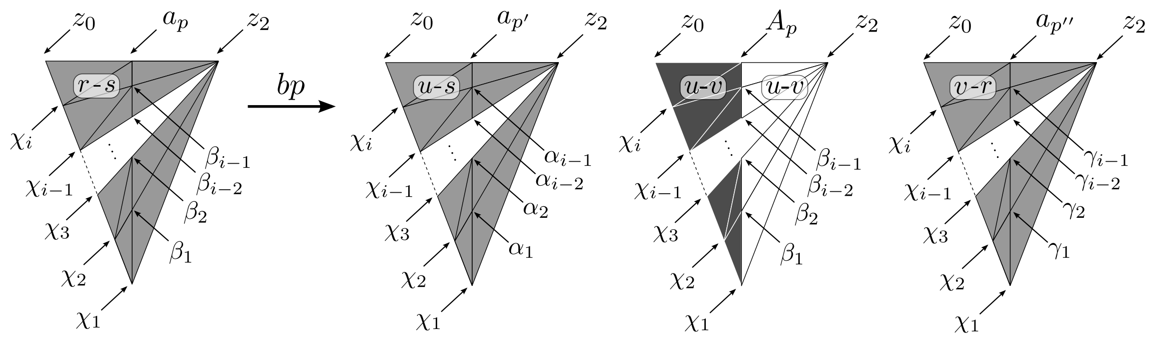

Figure 21: Embedding the part of the pillow corresponding to the tail of the balloon: case B_i' of the tail.

In this case, we need to reduce the PL3-faces ∇_r and ∇_s to create enough space to build PL2-faces 0- and 2-colored. To define 0-simplices α_j and γ_j, one of these cases is analogous to the case not refined, but the other we describe here. (∇_r is in the new case is the rank of PL2_0-face is equals to the rank of the PL2_1-face plus 2, if its not true, the new case is in the PL3-face ∇_v). Suppose that the new case is in the PL3-face, ∇_r. To define α_j, suppose that the PL2_0-face of this PL3-face is not refined, see Fig. 22. Define each α_j as the middle point between β_j and ω_j.

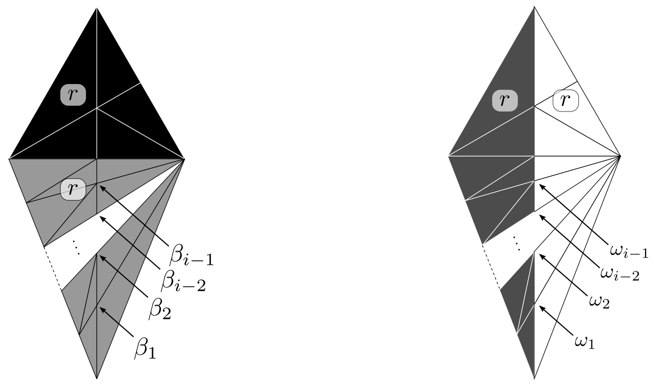

Figure 22: Using the PL3-face ∇_r to define α_j as $\frac{\omega_j+\beta_j}{2}$.

Consider the case that the PL2_0-face, of the PL3-face ∇_r, is refined see Fig. 23. This is a final subtlety which is treated with the *bump*. This is characterized by a non-convex pentagon shown in the bottom part of Fig. 23. Let ν_j be $\frac{z_2+\omega_j}{2}$ and α_j as $\frac{\beta_{j-1}+\nu_j}{2}$, for $j = 1, \ldots, i-1$. Observe that if we define α_j as if the PL2_0-face where not refined, some 1-simplices may cross.

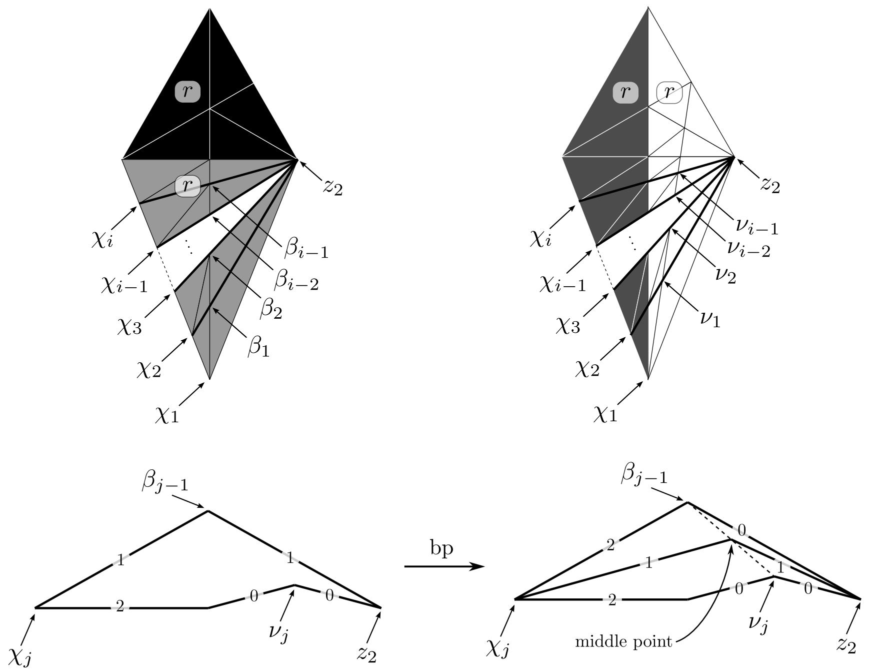

Figure 23: The bump: a final subtlety and how to deal with it.

□

References

[1] É. Colin de Verdière, M. Pocchiola, and G. Vegter. Tutte's barycenter method applied to isotopies. *Computational Geometry*, 26(1):81–97, 2003.

[2] Thomas H Cormen, Charles E Leiserson, Ronald L Rivest, and Clifford Stein. *Introduction to Algorithms*. MIT press, 2001.

[3] M. Ferri and C. Gagliardi. Crystallisation moves. *Pacific J. Math*, 100(1):85–103, 1982.

[4] S. Lins. A simple proof of Gagliardi's handle recognition theorem. *Discrete mathematics*, 57(3):253–260, 1985.

[5] S. Lins. On the fundamental group of 3-gems and a planar class of 3-manifolds. *European Journal of Combinatorics*, 9(4):291–305, 1988.

[6] S. Lins and A. Mandel. Graph-encoded 3-manifolds. *Discrete Math.*, 57(3):261–284, 1985.

[7] S. Lins and M. Mulazzani. Blobs and flips on gems. *Journal of Knot Theory and its Ramifications*, 15(8):1001–1035, 2006.

[8] S. L. Lins. *Gems, Computers, and Attractors for 3-Manifolds*. World Scientific, 1995.

[9] S. L. Lins and R. N. Machado. Framed link presentations of 3-manifolds by an $O(n^2)$ algorithm, I: gems and their duals. *arXiv:1211.1953v2 [math.GT]*, 2012.

[10] S. L. Lins and R. N. Machado. Framed link presentations of 3-manifolds by an $O(n^2)$ algorithm, II: colored complexes and boundings in their complexity. *arXiv:1212.0826v2 [math.GT]*, 2012.

[11] S. L. Lins and R. N. Machado. Framed link presentations of 3-manifolds by an $O(n^2)$ algorithm, III: geometric complex $\mathcal{H}_n^\star$ embedded into $\mathbb{R}^3$. *arXiv:1212.0827v2 [math.GT]*, 2012.

[12] C.P. Rourke and B.J. Sanderson. *Introduction to piecewise-linear topology*, volume 69. Springer-Verlag, 1982.

[13] J. Stillwell. *Classical Topology and Combinatorial Group Theory*. Springer Verlag, 1993.

[14] W. T. Tutte. How to draw a graph. *Proc. London Math. Soc*, 13(3):743–768, 1963.

Sóstenes L. Lins
Centro de Informática, UFPE
Av. Jornalista Aníbal Fernandes s/n
Recife–PE 50740-560
Brazil
sostenes@cin.ufpe.br

Ricardo N. Machado
Núcleo de Formação de Docentes, UFPE
Av. Jornalista Aníbal Fernandes s/n
Caruaru–PE
Brazil
ricardonmachado@gmail.com